containing exons of the *p53* gene amplified by the polymerase chain reaction (PCR) method. The singly ^{32}P-5′-end-labeled 443 bp fragment (*Apa*I 14179–*Eco*RI* 14621) was obtained according to the method described previously [17]. DNA fragment of the human c-Ha-*ras*-1 protooncogene was prepared from plasmid pbcNI, which carries a 6.6 kb *Bam*HI chromosomal DNA segment containing the c-Ha-*ras*-1 gene. The singly labeled 337 bp fragment (*Pst*I 2345–*Ava*I* 2681) was obtained according to the method described previously [18]. Nucleotide numbering starts with the *Bam*HI site [16]. Exon-containing DNA fragments were also obtained from the human *p16* tumor suppressor gene [15]; these fragments were subcloned into the pGEM®-T Easy Vector (Promega Corporation). The 484 bp fragment was further digested with *Bss*HII to obtain a singly labeled 156 bp fragment (*Bss*HII 9794–*Eco*RI* 9949) and a 324 bp fragment (*Eco*RI* 9466–*Bss*HII 9789). The asterisk indicates ^{32}P-labeling.

2.3. Detection of DNA damage by eugenol treated with CYP in the presence of metal ion

Standard reaction mixtures (in a 1.5 ml Eppendorf microtube) containing eugenol, various concentrations of CYP isozyme and NADPH-generating system (200 μM $NADP^+$, 500 μM G-6-P, 0.07 units G-6-PDH and 500 μM $MgCl_2$) in 200 μL of 10 mM sodium phosphate buffer (pH 7.8) containing 5 μM DTPA were preincubated for 1 h at 37 °C. After preincubation, [^{32}P]-5′-end labeled DNA fragments, calf thymus DNA (20 μM/base) and 20 μM $CuCl_2$ were added to the mixtures, followed by the incubation for 1 h at 37 °C. Subsequently, the DNA was treated with 1 M piperidine for 20 min at 90 °C or 10 units of Fpg protein in the reaction buffer (10 mM HEPES–KOH (pH 7.4), 100 mM KCl, 10 mM EDTA and 0.1 mg/mL BSA) for 2 h at 37 °C. Fpg protein catalyzes the excision of 8-oxodG as well as Fapy residues [19–21]. After ethanol precipitation, the DNA fragments were electrophoresed and the autoradiogram was obtained by exposing X-ray film to the gel as described previously [22]. The preferred cleavage sites were determined by direct comparison of the positions of the oligonucleotides with those produced by the chemical reactions of the Maxam–Gilbert procedure [23] using a DNA-sequencing system (LKB 2010 Macrophor). A laser densitometer (LKB 2222 UltroScan XL) was used for the measurement of the relative amounts of oligonucleotides from the treated DNA fragments.

2.4. Analysis of 8-oxodG formation in calf thymus DNA by eugenol treated with CYP2D6

The quantity of 8-oxodG was measured utilizing a modification of the method described by Kasai et al. [24]. Standard reaction mixtures (in a 2.0 ml Eppendorf microtube) containing eugenol, 0.25 nM CYP2D6, 200 μM $NADP^+$, 500 μM G-6-P, 0.20 units G-6-PDH and 500 μM $MgCl_2$ in 400 μL of 4 mM sodium phosphate buffer (pH 7.8) containing 5 μM DTPA were preincubated for 1 h at 37 °C. And then, calf thymus DNA (100 μM/base) and 20 μM $CuCl_2$ were added to the mixtures, followed by the incubation for 1 h at 37 °C. Following ethanol precipitation, the DNA fragments were digested into the nucleosides with nuclease P_1 and calf intestine phosphatase, and then analyzed by HPLC–ECD, as described previously [25].

2.5. TOF-MS analysis

TOF-MS analysis was performed on a Voyager B-RP (PerSeptive Biosystems, Framingham, MA) equipped with a nitrogen laser (337 nm, 3 ns pulse) to determine the molecular weight of eugenol metabolites generated by CYP2D6 treatment. Reaction mixture, containing 50 mM eugenol, 2.8 nM CYP2D6, 200 μM $NADP^+$, 2.5 mM G-6-P, 2.0 units G-6-PDH and 5 mM $MgCl_2$ in 100 μL of 10 mM sodium phosphate buffer (pH 7.8) were incubated for 1 h at 37 °C, and then air-dried on a stainless-steel probe tip. α-Cyano-4-hydroxycinnamic acid solution was added to the sample.

3. Results

3.1. Damage to [^{32}P]-labeled DNA fragments by eugenol treated with various CYP isozymes in the presence of metal ions

Eugenol treated with CYP induced Cu(II)-mediated DNA damage (Fig. 1). CYP2D6 mediated eugenol-induced DNA damage more efficiently than CYP 1A1, 1A2, 2C9 and 2E1 (Fig. 1A). CYP2D6-treated eugenol induced an increase of DNA damage in a

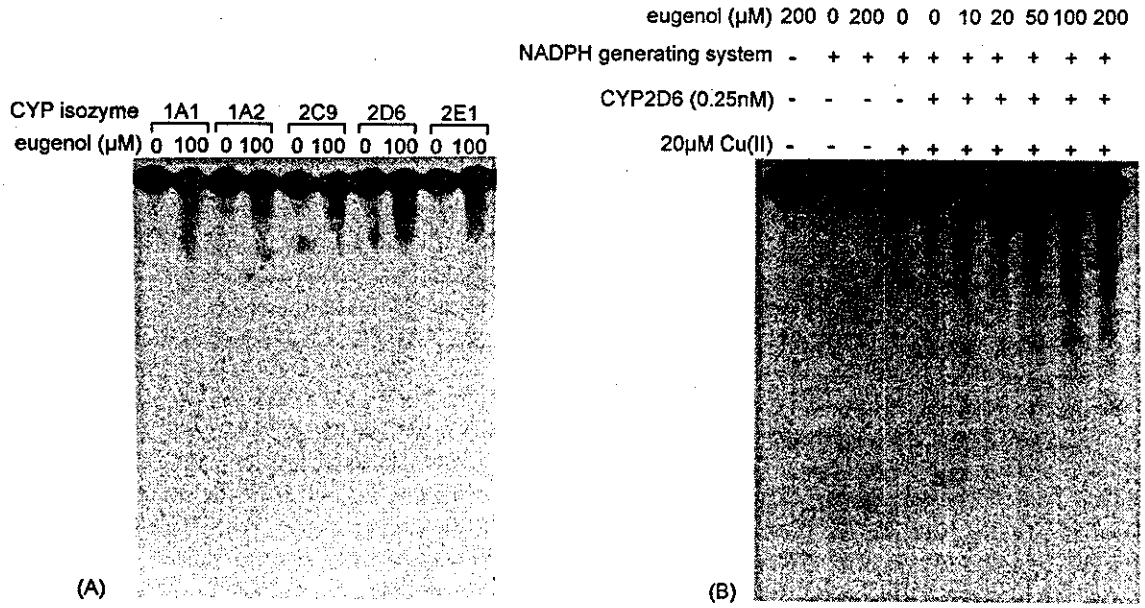

Fig. 1. Autoradiogram of ^{32}P-labeled DNA fragments incubated with CYP-treated eugenol plus Cu(II). (A) The reaction mixtures containing indicated no or 100 μM eugenol, 0.25 nM CYP 1A1, 1A2, 2C9, 2D6 or 2E1 and NADPH-generating system (200 μM $NADP^+$, 500 μM G-6-P, 0.07 units G-6-PDH and 500 μM $MgCl_2$) in 200 μL of 10 mM sodium phosphate buffer (pH 7.8) containing 5 μM DTPA were preincubated for 1 h at 37 °C. After preincubation, ^{32}P-5′-end labeled DNA fragments, calf thymus DNA (20 μM/base) and 20 μM $CuCl_2$ were added to the preincubated mixtures. (B) The reaction mixtures containing indicated concentrations of eugenol and NADPH-generating system in 200 μL of 10 mM sodium phosphate buffer (pH 7.8) containing 5 μM DTPA were preincubated for 1 h at 37 °C. After preincubation, ^{32}P-5′-end labeled DNA fragments, calf thymus DNA (20 μM/base) and 20 μM $CuCl_2$ were added to the mixtures, followed by the incubation for 1 h at 37 °C. Subsequently, DNA fragments were treated with 1 M piperidine for 20 min at 90 °C, then electrophoresed on an 8% polyacrylamide/8 M urea gel. The autoradiogram was visualized by exposing an X-ray film to the gel.

dose-dependent manner (Fig. 1B). DNA damage was enhanced by piperidine treatment, suggesting that eugenol caused not only DNA strand breakage but also base modification (data not shown). Without CYP treatment, eugenol did not induce DNA damage (Fig. 1B). The treated eugenol did not induce DNA damage in the presence of other metal ions, including Co(II), Ni(II), Mn(II), Mn(III), Fe(II), Fe(III) or Fe(III)EDTA (data not shown).

3.2. Effects of scavengers and a metal chelator on DNA damage induced by eugenol treated with CYP2D6

Fig. 2 shows the effects of scavengers and a metal chelator on Cu(II)-mediated DNA damage induced by eugenol in the presence of CYP2D6. Catalase and bathocuproine inhibited DNA damage, suggesting the involvement of H_2O_2 and Cu(I). Free hydroxyl radical (•OH) scavengers, such as ethanol, mannitol, sodium formate and DMSO, showed little or no inhibitory effect on DNA damage. Methional, which is capable of scavenging both •OH and species with weaker reactivity such as Cu(I)–hydroperoxo complex [26], inhibited DNA damage. SOD showed no inhibitory effect on DNA damage.

3.3. Site specificity of DNA cleavage by eugenol treated with CYP2D6

The patterns of DNA cleavage induced by eugenol in the presence of Cu(II) and CYP2D6 were determined by the Maxam–Gilbert procedure [23]. An autoradiogram was obtained and scanned with a laser densitometer to measure relative intensity of DNA cleavage in the human *p53* tumor suppressor gene (Fig. 3A and B). The treated eugenol caused piperidine-labile and Fpg sensitive lesions at C and G in the 5′-ACG-3′ sequence,

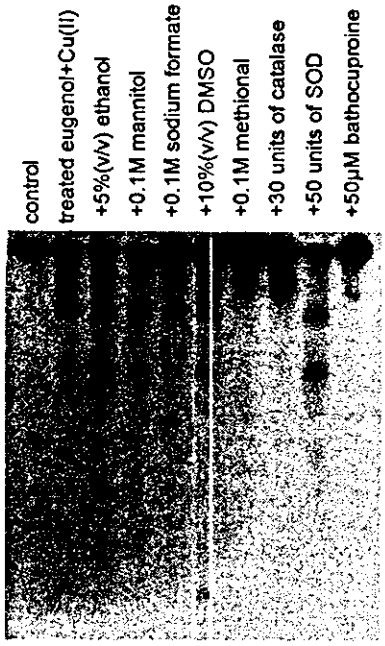

Fig. 2. Effects of scavengers and bathocuproine on DNA damage induced by eugenol treated with CYP2D6 in the presence of Cu(II). Reaction mixtures contained the ^{32}P-5′-end-labeled 211-bp DNA fragment, 20 μM/base of calf thymus DNA, 20 μM eugenol treated with 0.25 nM CYP2D6 and 20 μM $CuCl_2$ in 200 μL of 10 mM sodium phosphate buffer (pH 7.8) containing 5 μM DTPA. Reaction mixtures were incubated for 1 h at 37 °C. DNA fragments were treated with 1 M piperidine for 20 min at 90 °C, then electrophoresed on an 8% polyacrylamide/8 M urea gel. The autoradiogram was visualized by exposing an X-ray film to the gel.

a well-known hotspot of the *p53* gene, respectively (Fig. 3A). With Fpg treatment, the DNA cleavage occurred mainly at guanine and cytosine residues. In addition, tandem two bases of 5′-TG-3′ site were often damaged together with Fpg and piperidine treatment (Fig. 3B). From these results, it is considered that the treated eugenol can cause double base lesions at 5′-TG-3′ and 5′-CG-3′ sequences at high frequency.

3.4. Formation of 8-oxodG in calf thymus DNA by eugenol treated with CYP2D6 in the presence of Cu(II)

Using an HPLC–ECD, we measured the quantity of 8-oxodG, an indicator of oxidative base damage [24], in calf thymus DNA treated with eugenol in the presence of Cu(II) and CYP2D6. The treated eugenol induced an increase of 8-oxodG formation in a dose dependent manner (Fig. 4). Heat-inactivated CYP2D6 did not increase the eugenol-dependent 8-oxodG formation.

3.5. Production of O-demethyl eugenol from eugenol treated with CYP2D6

Fig. 5 shows mass spectra of eugenol without (A) and with (B) CYP2D6 treatment. Without treatment, eugenol showed the mass spectrum with molecular ion at *m/e* 164 (M) (Fig. 5A). The metabolite obtained from the reaction mixture of eugenol and CYP2D6 showed the mass spectrum with molecular ion at *m/e* 151 (*M* + 1), which is assigned to *O*-hydroxychavicol (Fig. 5B). This result suggests that CYP2D6 catalyzes *O*-demethylation of eugenol to produce hydroxychavicol.

4. Discussion

Since there are a lot of CYPs in liver, we investigated the possibility that eugenol is metabolized to ultimate carcinogen causing DNA damage in the liver. The present study has demonstrated that CYP2D6 mediates eugenol-dependent DNA damage in the presence of Cu(II). When CYP1A1, CYP1A2 and CYP2E1 were added instead of CYP2D6, DNA damage was similarly observed to a lesser extent. Experiments with piperidine or Fpg treatment revealed that C and G of the 5′-ACG-3′ sequence, the complementary sequence to codon 273 (a known hotspot) in exon 8 of the *p53* gene [12,27], were significantly damaged. Eugenol treated with CYP 2D6 also formed piperidine-labile and Fpg-sensitive lesions at T and G of the 5′-TG-3′ sequence, respectively. Fpg protein mainly catalyzes the excision of piperidine-resistant 8-oxodG [19] and further oxidized piperidine-labile guanine residues [28], although Fpg also mediates cleavage of uracil glycol [29], 5-hydroxycytosine and 5,6-dihydrothymine [30] in vitro. Therefore, it is reasonably considered that the treated eugenol oxidizes the G residue of 5′-CG-3′ and 5′-TG-3′ sequences to 8-oxodG. It has been reported that reactive oxygen species induced double base lesions to DNA oligomers [31,32]. Such clustered damage, including double base lesions, appears to play an important role in carcinogenesis, because clustered damage, which can be demonstrated in living cells, is poorly repaired [33].

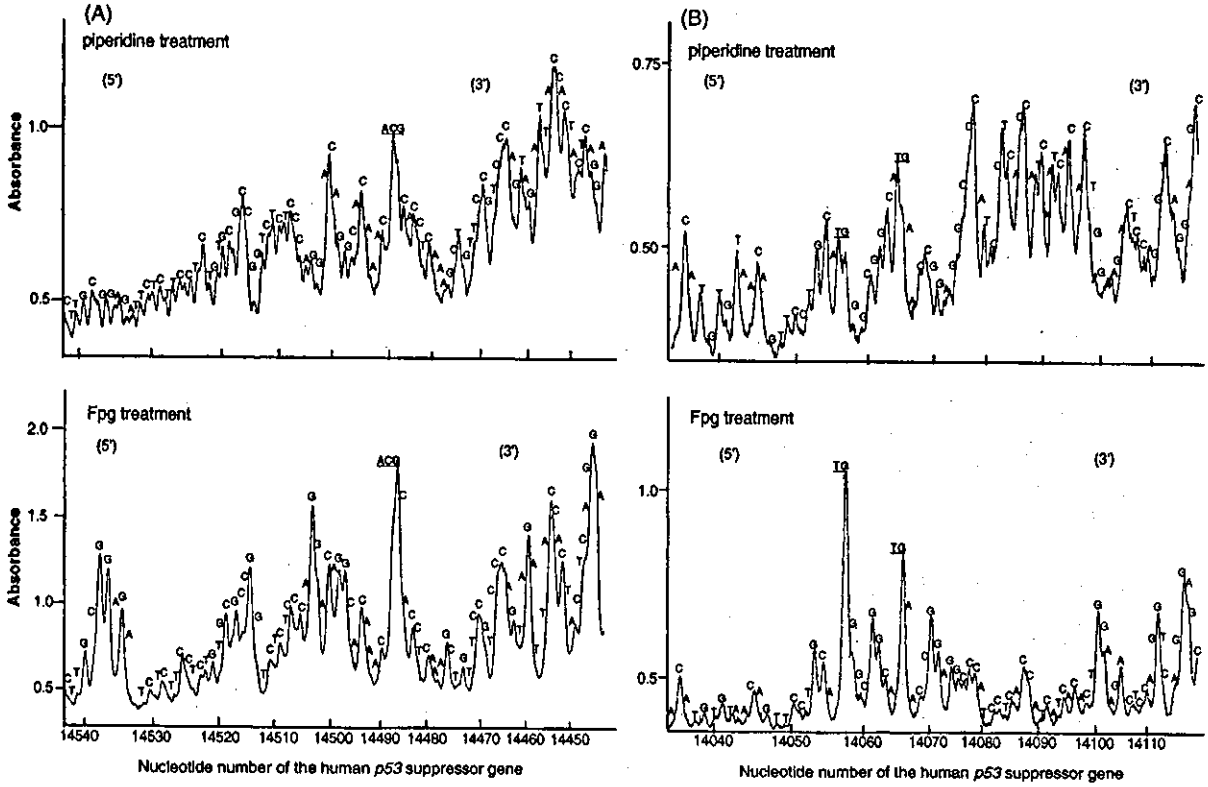

Fig. 3. Site specificity of DNA cleavage induced by eugenol treated with CYP2D6 in the presence of Cu(II). Reaction mixtures contained either the ^{32}P-5'-end-labeled 443 bp fragment (*Apa*I 14179–*Eco*RI* 14621) (A) or the 211 bp fragment (*Hin*dIII* 13972–*Apa*I 14182) (B) derived from the *p53* tumor suppressor gene, 20 μM/base of calf thymus DNA, 200 μM eugenol treated with 0.25 nM CYP2D6 and 20 μM $CuCl_2$ in 200 μL of 10 mM sodium phosphate buffer (pH 7.8) containing 5 μM DTPA. Reaction mixtures were incubated for 1 h at 37 °C. Following piperidine or Fpg treatment, the DNA fragments were analyzed as described in Fig. 1(legend). The relative quantities of oligonucleotides were measured by scanning the autoradiogram with a laser densitometer (LKB 2222 UltroScan XL, Pharmacia Biotech). Underlined bases represent double-base lesions detected by the treatment with piperidine and Fpg protein.

In addition, time-of-flight-mass spectrometry demonstrated that CYP2D6 catalyzed the *O*-demethylation of eugenol to produce hydroxychavicol. Hydroxychavicol appears to be the ultimate carcinogen, capable of causing DNA damage. This result is supported by reports that CYP2D6 as well as CYP 1A1, CYP1A2 and CYP2E1 can catalyze *O*-demethylation reactions [34–36].

To clarify what kind of the reactive species involved in DNA damage by eugenol treated with CYP2D6, we examined the effects of scavengers on DNA damage. The inhibitory effect of catalase suggests the involvement of H_2O_2. The observed protective effect of bathocuproine suggests that Cu(I) is required for DNA damage. This is supported by reports that bathocuproine inhibits the activation of H_2O_2 by stabilizing Cu(I) [37,38]. Typical •OH scavengers demonstrated little or no inhibitory effect, whereas methional inhibited DNA damage. This result suggests the involvement of reactive species with a similar reactivity to •OH [26]. Therefore, it is considered that reactive species such as Cu(I)–hydroperoxo complex obtained with H_2O_2 and Cu(I) are involved in DNA damage by CYP2D6-treated eugenol. However, •OH may participate in DNA damage through the formation of the DNA–Cu(I)–hydroperoxo complex, which releases •OH to attack the adjacent DNA constituents prior to being scavenged by •OH scavengers [39].

On the basis of these data, we propose a possible mechanism by which eugenol induces Cu(II)-mediated

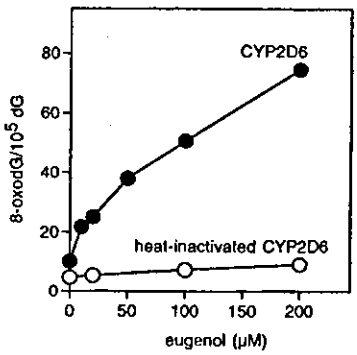

Fig. 4. Formation of 8-oxodG by eugenol treated with CYP2D6 in the presence of Cu(II). Standard reaction mixtures containing eugenol, 0.25 nM CYP2D6 and NADPH-generating system (200 μM $NADP^+$, 500 μM G-6-P, 0.07 units G-6-PDH and 500 μM $MgCl_2$) in 400 μL of 4 mM sodium phosphate buffer (pH 7.8) containing 5 μM DTPA were preincubated for 2 h at 37 °C. And then, calf thymus DNA (100 μM/base) and 20 μM $CuCl_2$were added to the mixtures. Following incubation for 1 h at 37 °C, 0.2 mM DTPA was added to stop the reaction and then the DNA was precipitated in ethanol. In certain experiments, CYP2D6 and NADPH-generating system were heated at 90 °C for 30 min for inactivation before the preincubation. The DNA was subjected to enzymatic digestion and analyzed by HPLC–ECD.

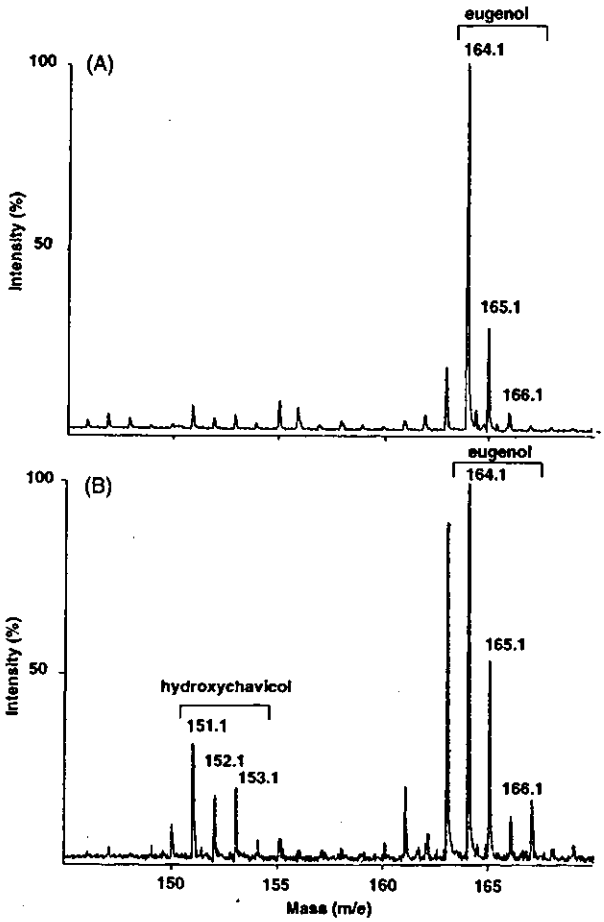

Fig. 5. Production of *O*-demethyleugenol from eugenol treated with CYP2D6. Reaction mixture, containing 50 mM eugenol, 2.8 nM CYP2D6, 200 μM $NADP^+$, 2.5 mM G-6-P, 2.0 units G-6-PDH and 5 mM $MgCl_2$ in 200 μL of 10 mM sodium phosphate buffer (pH 7.8) were incubated for 1 h at 37 °C, and then air-dried on a stainless-steel probe tip. α-Cyano-4-hydroxycinnamic acid solution was added to the sample. TOF-MS analysis was performed on a Voyager B-RP (PerSeptive Biosystems, Framingham, MA) equipped with a nitrogen laser (337 nm, 3 ns pulse). (A) No treated eugenol; (B) CYP2D6-treated eugenol.

DNA damage (Fig. 6). Eugenol undergoes certain CYPs-catalyzed *O*-demethylation to hydroxychavicol, a catechol derivative. Hydroxychavicol is then autoxidized into the semiquinone radical, leading to the production of the corresponding *o*-quinone form. Cu(II) is reduced to Cu(I) during the autoxidation, and O_2^- is concomitantly generated, followed by dismutation to H_2O_2. It has been also reported that hydroxychavicol produces superoxide radicals and H_2O_2 [40]. H_2O_2 interacts with Cu(I) to form the Cu(I)–hydroperoxo complex, capable of inducing DNA damage [41]. Several studies indicate that NAD(P)H may non-enzymatically reduce *o*-quinones to catechols through two-electron reduction [42]. Tissue concentrations of NAD(P)H can be as high as 100 μM [43,44]. Thus, the NADH-dependent redox cycle of hydroxychavicol may continuously generate reactive oxygen species and mediate enhancement of oxidative DNA damage.

In summary, we have demonstrated that a eugenol metabolite, hydroxychavicol, can cause oxidative DNA damage, probably double base lesions at 5′-CG-3′ and 5′-TG-3′ sequences. G residue in these sequences was oxidized to 8-oxodG, which might lead to mutation (G:C → T:A transversion) through the misreplication of DNA [45–47]. Finally, eugenol and methyleugenol may cause carcinogenesis through oxidative DNA damage in addition to DNA adduct. Further study on safety should be required when eugenol and its derivatives is used for a flavoring agent, fragrance and an analgesic.

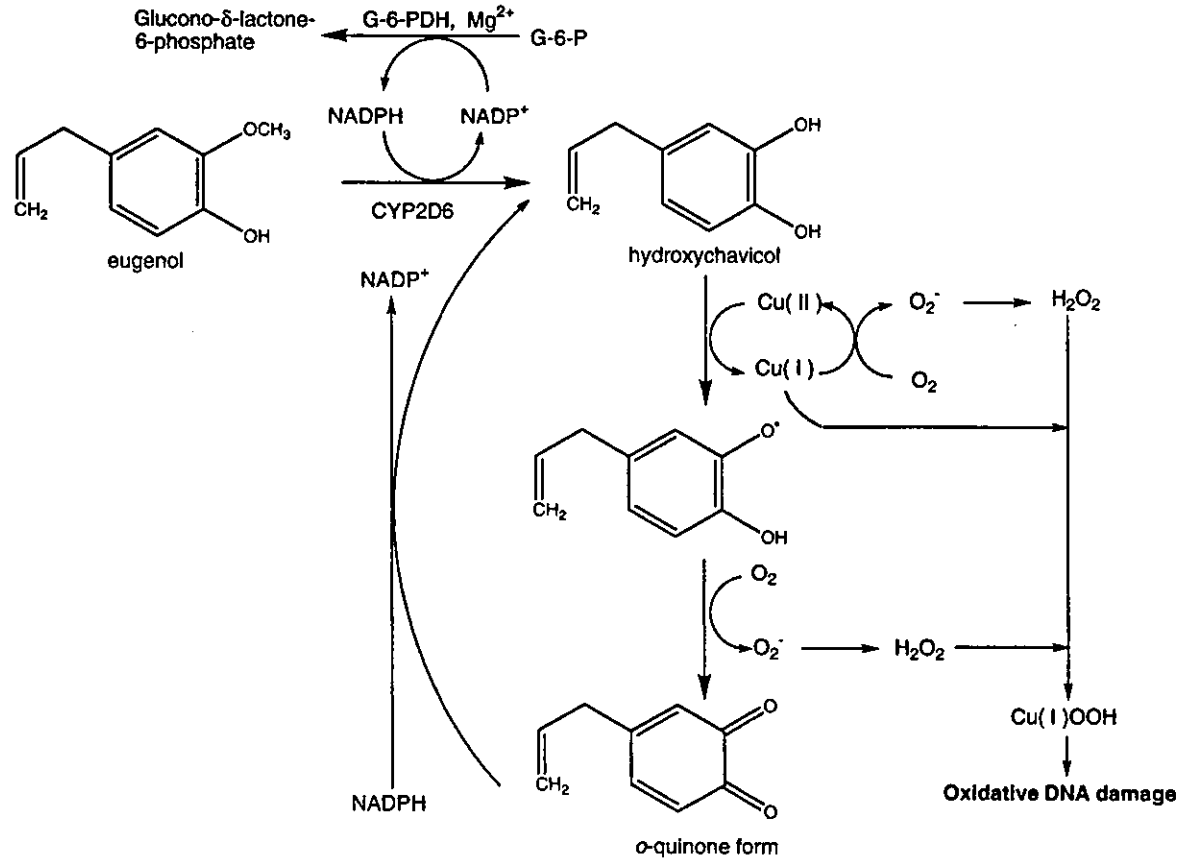

Fig. 6. A possible mechanism for Cu(II)-mediated DNA damage induced by eugenol in the presence of CYP2D6.

References

[1] IARC Monographs, Eugenol, vol. 36, International Agency for Research on Cancer, Lyon, France, 1985, pp. 75–97.
[2] Council on Scientific Affairs American Medical Association, Evaluation of the health hazards of clove cigarettes, in: Proceedings of the House of Delegates, 1988, pp. 319–325.
[3] S.S. Kim, O.-J. Oh, H.-Y. Min, E.-J. Park, Y. Kim, H.J. Park, Y.N. Han, S.K. Lee, Eugenol suppresses cyclooxygenase-2 expression in lipopolysaccharide-stimulated mouse macrophage RAW264.7 cells, Life Sci. 73 (2003) 337–348.
[4] C.J. Rompelberg, J.T. Vogels, N. de Vogel, G.C. Bruijntjes-Rozier, W.H. Stenhuis, J.J. Bogaards, H. Verhagen, Effect of short-term dietary administration of eugenol in humans, Hum. Exp. Toxicol. 15 (2) (1996) 129–135.
[5] C.J. Rompelberg, W.H. Stenhuis, N. de Vogel, W.A. van Osenbruggen, A. Schouten, H. Verhagen, Antimutagenicity of eugenol in the rodent bone marrow micronucleus test, Mutat. Res. 346 (2) (1995) 69–75.
[6] K. Sukumaran, R. Kuttan, Inhibition of tobacco-induced mutagenesis by eugenol and plant extracts, Mutat. Res. 343 (1) (1995) 25–30.
[7] C.J. Woolverton, P.G. Fotos, M.J. Mokas, M.E. Mermigas, Evaluation of eugenol for mutagenicity by the mouse micronucleus test, J. Oral. Pathol. 15 (1986) 450–453.
[8] H.F. Stitch, W. Stitch, P.P.S. Lam, Potentiation of genotoxicity by concurrent application of compounds found in betel quid: arecoline, eugenol, quercetine, chlorogenic acid and Mn^{2+}, Mutat. Res. 90 (1981) 355–363.
[9] National Toxicology Program, NTP Toxicology and Carcinogenesis Studies of Methyleugenol (CAS No. 93-15-2), in: F344/N Rats and B6C3F1 Mice (Gavage Studies), Natl. Toxicol. Prog. Tech. Rep. Ser. 491 (2000 July) 1–412.
[10] T.M. F. Guenthner, G. Luo, Investigation of the role of the 2′,3′-epoxidation pathway in the bioactivation and genotoxicity of dietary allylbenzene analogs, Toxicology 160 (1–3) (2001) 47–58.
[11] W.J. Bodell, Q. Ye, D.N. Pathak, K. Pongrcz, Oxidation of eugenol to form DNA adducts and 8-hydroxy-2-deoxyguanosine: role of quinone methide derivative in DNA adduct formation, Carcinogenesis 19 (1998) 437–444.

[12] M.F. Denissenko, A. Pao, M. Tang, G.P. Pfeifer, Preferential formation of benzo[*a*]pyrene adducts at lung cancer mutational hotspots in *P53*, Science 274 (5286) (1996) 430–432.
[13] S.J. Wei, R.L. Chang, K.A. Merkler, M. Gwynne, X.X. Cui, B. Murthy, M.T. Huang, J.G. Xie, Y.P. Lu, Y.R. Lou, D.M. Jerina, A.H. Conney, Dose-dependent mutation profile in the c-Ha-*ras* proto-oncogene of skin tumors in mice initiated with benzo[*a*]pyrene, Carcinogenesis 9 (1999) 1689–1696.
[14] P. Chumakov, EMBL Data Library, accession number X54156, 1990.
[15] M. Serrano, G.J. Hannon, D. Beach, A new regulatory motif in cell-cycle control causing specific inhibition of cyclin D/CDK4, Nature 366 (6456) (1993) 704–707.
[16] D.J. Capon, P.H. Seeburg, J.P. McGrath, J.S. Hayflick, U. Edman, A.D. Levinson, D.V. Goeddel, Activation of *Ki-ras2* gene in human colon and lung carcinomas by two different point mutations, Nature 304 (5926) (1983) 507–513.
[17] N. Yamashita, M. Murata, S. Inoue, Y. Hiraku, T. Yoshinaga, S. Kawanishi, Superoxide formation and DNA damage induced by a fragrant furanone in the presence of copper(II), Mutat. Res. 397 (2) (1998) 191–201.
[18] K. Yamamoto, S. Kawanishi, Hydroxyl free radical is not the main active species in site-specific DNA damage induced by copper(II) ion and hydrogen peroxide, J. Biol. Chem. 264 (26) (1989) 15435–15440.
[19] M.H. David-Cordonnier, J. Laval, P. O'Neill, Clustered DNA damage, influence on damage excision by XRS5 nuclear extracts and *Escherichia coli* Nth and Fpg proteins, J. Biol. Chem. 275 (16) (2000) 11865–11873.
[20] S. Boiteux, E. Gajewski, J. Laval, M. Dizdaroglu, Substrate specificity of the *Escherichia coli* Fpg protein (formamidopyrimidine-DNA glycosylase): excision of purine lesions in DNA produced by ionizing radiation or photosensitization, Biochemistry 31 (1) (1992) 106–110.
[21] S.D. Bruner, D.P. Norman, G.L. Verdine, Structural basis for recognition and repair of the endogenous mutagen 8-oxoguanine in DNA, Nature 403 (6772) (2000) 859–866.
[22] S. Oikawa, S. Kawanishi, in: N. Taniguchi, M.G.J. Gutteridge (Eds.), Detection of DNA damage and analysis of its site-specificity, Oxford University Press, New York, 2000, pp. 229–235.
[23] A.M. Maxam, W. Gilbert, Sequencing end-labeled DNA with base-specific chemical cleavages, Methods Enzymol. 65 (1) (1980) 499–560.
[24] H. Kasai, P.F. Crain, Y. Kuchino, S. Nishimura, A. Ootsuyama, H. Tanooka, Formation of 8-hydroxyguanine moiety in cellular DNA by agents producing oxygen radicals and evidence for its repair, Carcinogenesis 7 (11) (1986) 1849–1851.
[25] K. Ito, S. Inoue, K. Yamamoto, S. Kawanishi, 8-Hydroxydeoxyguanosine formation at the 5′ site of 5′-GG-3′ sequences in double-stranded DNA by UV-radiation with riboflavin, J. Biol. Chem. 268 (18) (1993) 13221–13227.
[26] R.J. Youngman, E.F. Elstner, Oxygen species in paraquat toxicity: the crypto-OH radical, FEBS Lett. 129 (2) (1981) 265–268.
[27] M. Hollstein, D. Sidransky, B. Vogelstein, C.C. Harris, *p53* mutations in human cancers, Science 253 (1991) 49–53.
[28] D. Gasparutto, J.L. Ravanat, O. Gérot, J. Cadet, Characterization and chemical stability of photooxidized oligonucleotides that contain 2,2-diamino-4-[(2-deoxy-β-D-*erythro*-pentofuranosyl)amino]-5(2*H*)-oxazolone, J. Am. Chem. Soc. 120 (1998) 10283–10286.
[29] A.A. Purmal, G.W. Lampman, J.P. Bond, Z. Hatahet, S.S. Wallace, Enzymatic processing of uracil glycol, a major oxidative product of DNA cytosine, J. Biol. Chem. 273 (1998) 10026–10035.
[30] C. D'Ham, A. Romieu, M. Jaquinod, D. Gasparutto, J. Cadet, Excision of 5,6-dihydroxy-5,6-dihydrothymine, 5,6-dihydrothymine, and 5-hydroxycytosine from defined sequence oligonucleotides by *Escherichia coli* endonuclease III and Fpg proteins: kinetic and mechanistic aspects, Biochemistry 38 (1998) 3335–3344.
[31] H.C. Box, J.B. Dawidzik, E.E. Budzinski, Free radical-induced double lesions in DNA, Free Radic. Biol. Med. 31 (2001) 856–868.
[32] A.G. Bourdat, T. Douki, S. Frelon, D. Gasparutto, J. Cadet, Tandem base lesions are generated by hydroxyl radical within isolated DNA in aerated aqueous solution, J. Am. Chem. Soc. 122 (2000) 4549–4556.
[33] J.O. Blaisdell, S.S. Wallace, Abortive base-excision repair of radiation-induced clustered DNA lesions in *Escherichia coli*, Proc. Natl. Acad. Sci. U.S.A. 98 (2001) 7426–7430.
[34] N. Chauret, B. Dobbs, R.L. Lackman, K. Bateman, D.A. Nicoll-Griffith, D.M. Stresser, J.M. Ackermann, S.D. Turner, V.P. Miller, C.L. Crespi, The use of 3-[2-(*N*,*N*-diethyl-*N*-methylammonium)ethyl]-7-methoxy-4-methylcoumarin (AMMC) as a specific CYP2D6 probe in human liver microsomes, Drug Metab. Dispos. 29 (9) (2001) 1196–1200.
[35] Y.J. Chun, M.Y. Kim, F.P. Guengerich, Resveratrol is a selective human cytochrome P4501A1 inhibitor, Biochem. Biophys. Res. Commun. 262 (1) (1999) 20–24.
[36] D.M. Stresser, D. Kupfer, Human cytochrome P450-catalyzed conversion of the proestrogenic pesticide methoxychlor into an estrogen: role of CYP2C19 and CYP1A2 in *O*-demethylation, Drug Metab. Dispos. 26 (9) (1998) 868–874.
[37] M.J. Burkitt, A critical overview of the chemistry of copper-dependent low-density lipoprotein oxidation: roles of lipid hydroperoxides, α-tocopherol, thiols, and ceruloplasmin, Arch. Biochem. Biophys. 394 (1) (2001) 117–135.
[38] S.L. Jewett, A.M. Rocklin, M. Ghanevati, J.M. Abel, J.A. Marach, A new look at a time-worn system: oxidation of CuZn–SOD by H_2O_2, Free Radic. Biol. Med. 26 (7–8) (1999) 905–918.
[39] M. Dizdaroglu, O.I. Aruoma, B. Halliwell, Modification of bases in DNA by copper ion-1,10-phenanthroline complexes, Biochemistry 29 (36) (1990) 8447–8451.
[40] J.H. Jeng, Y.J. Wang, W.H. Chang, H.L. Wu, C.H. Li, B.J. Uang, J.J. Kang, J.J. Lee, L.J. Hahn, B.R. Lin, M.C. Chang, Reactive oxygen species are crucial for hydroxychavicol toxicity toward KB epithelial cells, Cell Mol. Life Sci. 61 (1) (2004) 83–96.
[41] S. Kawanishi, Y. Hiraku, S. Oikawa, Mechanism of guanine-specific DNA damage by oxidative stress and its role in carcinogenesis and aging, Mutat. Res. 488 (1) (2001) 65–76.

[42] K. Hirakawa, S. Oikawa, Y. Hiraku, I. Hirosawa, S. Kawanishi, Catechol and hydroquinone have different redox properties responsible for their differential DNA-damaging ability, Chem. Res. Toxicol. 15 (1) (2002) 76–82.
[43] A. Gaikwad, D.J. Long II, J.L. Stringer, A.K. Jaiswal, In vivo role of NAD(P)H:quinone oxidoreductase 1 (NQO1) in the regulation of intracellular redox state and accumulation of abdominal adipose tissue, J. Biol. Chem. 276 (25) (2001) 22559–22564.
[44] W.J. Malaisse, J.C. Hutton, S. Kawazu, A. Herchuelz, I. Valverde, A. Sener, The stimulus-secretion coupling of glucose-induced insulin release. XXXV. The links between metabolic and cationic events, Diabetologia 16 (5) (1979) 331–341.
[45] D.O. Zharkov, T.A. Rosenquist, S.E. Gerchman, A.P. Grollman, Substrate specificity and reaction mechanism of murine 8-oxoguanine-DNA glycosylase, J. Biol. Chem. 275 (2000) 28607–28617.
[46] S. Shibutani, M. Takeshita, A.P. Grollman, Insertion of specific bases during DNA synthesis past the oxidation-damaged base 8-oxodG, Nature 349 (1991) 431–434.
[47] K.C. Cheng, D.S. Cahill, H. Kasai, S. Nishimura, L.A. Loeb, 8-Hydroxyguanine, an abundant form of oxidative DNA damage, causes G→T and A→C substitutions, J. Biol. Chem. 267 (1992) 166–172.

DNA intrastrand cross-link at the 5′-GA-3′ sequence formed by busulfan and its role in the cytotoxic effect

Takuya Iwamoto,[1,2] Yusuke Hiraku,[1] Shinji Oikawa,[1] Hideki Mizutani,[1,2] Michio Kojima[2] and Shosuke Kawanishi[1,3]

[1]Department of Environmental and Molecular Medicine, Mie University School of Medicine and [2]Department of Pharmacy, Mie University Hospital, 2-174 Edobashi, Tsu, Mie 514-8507

(Received December 17, 2003/Revised February 18, 2004/Accepted March 5, 2004)

Busulfan (1,4-butanediol dimethanesulfonate) has been used widely for the treatment of patients with chronic myelogenous leukemia. Busulfan is bifunctional and thus may effectively induce DNA damage, which may play an important role in the cytotoxicity. In this study, we compared the cytotoxicity of bifunctional busulfan with that of monofunctional ethyl methanesulfonate (EMS) in human promyelocytic leukemia HL-60 cells. Busulfan showed a significant inhibitory effect on cell growth, whereas the cells grew in the presence of EMS. To clarify the mechanism of cytotoxicity of busulfan, we investigated DNA damage induced by busulfan using ^{32}P-5′-end-labeled DNA fragments obtained from the human *p16* tumor suppressor gene. Busulfan induced DNA damage dose-dependently, whereas EMS caused little DNA damage. DNA-sequencing experiments using piperidine and 3-methyladenine DNA glycosylase indicated that busulfan caused double-base lesions mainly at 5′-GA-3′ and, to a lesser extent, at 5′-GG-3′ sequences. Time of flight mass spectrometry confirmed that busulfan forms an intrastrand cross-link at the 5′-GA-3′ sequence, in addition to mono-alkylation. The mechanism and the role of cross-linking at the 5′-GA-3′ sequence are discussed in relation to the cytotoxicity induced by busulfan. (Cancer Sci 2004; 95: 454–458)

Some important anticancer drugs used in clinical practice are bifunctional alkylating agents, and their most important cellular target is believed to be DNA. These drugs are able to form cross-links with biological macromolecules, and such DNA cross-links may be the critical cytotoxic lesion.[1,2] The N7 and O6 positions of guanine and N3 position of adenine are known to be alkylation sites for a number of chemotherapeutic alkylating agents.[3,4] The most readily alkylated site in DNA is the guanine-N7 position.[4–6]

Busulfan [1,4-butanediol dimethanesulfonate, $CH_3SO_2O(CH_2)_4OSO_2CH_3$], which is a bifunctional alkylating agent, has been used widely for the treatment of patients with chronic myelogenous leukemia and also in conditioning regimens prior to bone marrow transplantation.[7] Busulfan has a higher biological activity than other dimethanesulfonates in hematopoietic stem cells.[8] This higher biological activity may be explained by its ability to cause DNA bis-alkylation. A chromatographic study suggested that busulfan produced cross-links in DNA through a guanine-guanine bridge,[9,10] but no distinction has been made as to whether this bridge represents an inter- or intrastrand cross-link. The previous study using isolated DNA showed that busulfan is less likely to form an interstrand cross-link than methylene dimethanesulfonate, which has a shorter carbon chain length.[11] Thus, the formation of intrastrand cross-links rather than interstrand cross-links may play a key role in the cytotoxicity. It is therefore important to study in more detail the mechanism of DNA cross-link formation by busulfan.

In this study, we compared the DNA-damaging ability of bifunctional busulfan and monofunctional ethyl methanesulfonate (EMS, $CH_3SO_2OC_2H_5$) and their cytotoxicity towards human promyelocytic leukemia HL-60 cells. We also investigated the site specificity of busulfan-induced DNA damage using ^{32}P-5′-end-labeled DNA fragments obtained from the human *p16* tumor suppressor gene. Furthermore, time-of-flight mass spectrometry (TOF-MS) was performed to identify the DNA cross-links formed by busulfan.

Materials and Methods

Materials. Restriction enzymes (*Eco*RI and *Bss*HII) and proteinase K were from Boehringer Mannheim GmbH (Mannheim, Germany). T_4 polynucleotide kinase was obtained from New England Biolabs (Beverly, MA). [γ-^{32}P]ATP (222 TBq/mmol) was from New England Nuclear (Boston, MA). Diethylenetriamine-*N,N,N′,N″,N‴*-pentaacetic acid (DTPA) was from Dojin Chemical Co. (Kumamoto). Busulfan, calf thymus DNA, 3-hydroxypicolinic acid and citric acid were from Sigma Chemical Co. (St. Louis, MO). Acrylamide, dimethylsulfoxide, bisacrylamide and piperidine were from Wako Pure Chemical Industries (Osaka). EMS and ethanol were from Nacalai Tesque, Inc. (Kyoto). Mouse 3-methyladenine DNA glycosylase (Aag) was obtained from Trevigen Inc. (Gaithersburg, MD).

Growth-inhibitory and cytotoxic effects of busulfan and EMS on cultured cells. HL-60 cells (2.5×10^5 cells/ml) were incubated with 100 or 200 μM busulfan or 200 μM EMS in 2 ml of RPMI 1640 (Gibco Laboratories, NY) supplemented with 6% fetal calf serum (FCS, Whittaker Bioproducts) for 24 h at 37°C. Cell viability was determined by trypan blue exclusion and counting in a hemocytometer. For statistical analysis of the data, an independent *t* test was used, and the criterion of significance was set at $P<0.05$. The data represent means±SD of four independent experiments.

Preparation of ^{32}P-5′-end-labeled DNA fragments from the human *p16* gene. DNA fragments were prepared from the human *p16* tumor suppressor gene.[12] The ^{32}P-5′-end-labeled 484-base-pair fragment (*Eco*RI* 9466-*Eco*RI* 9949) was digested with *Bss*HII to obtain the singly labeled 324-base-pair (*Eco*RI* 9466-*Bss*HII 9789) and 156-base-pair (*Bss*HII 9794-*Eco*RI* 9949) DNA fragments as described previously.[13] The asterisk indicates ^{32}P-labeling.

Detection of DNA damage induced by busulfan and EMS. The standard reaction mixture (in a 1.5 ml Eppendorf microtube) contained busulfan or EMS, ^{32}P-end-labeled DNA fragments, and calf thymus DNA (2 μM/base) in 200 μl of 10 mM sodium

[3]To whom correspondence should be addressed.
E-mail: kawanisi@doc.medic.mie-u.ac.jp

Abbreviations: EMS, ethyl methanesulfonate; TOF-MS, time-of-flight mass spectrometry; DTPA, diethylenetriamine-*N,N,N′,N″,N‴*-pentaacetic acid; Aag, 3-methyladenine DNA glycosylase.

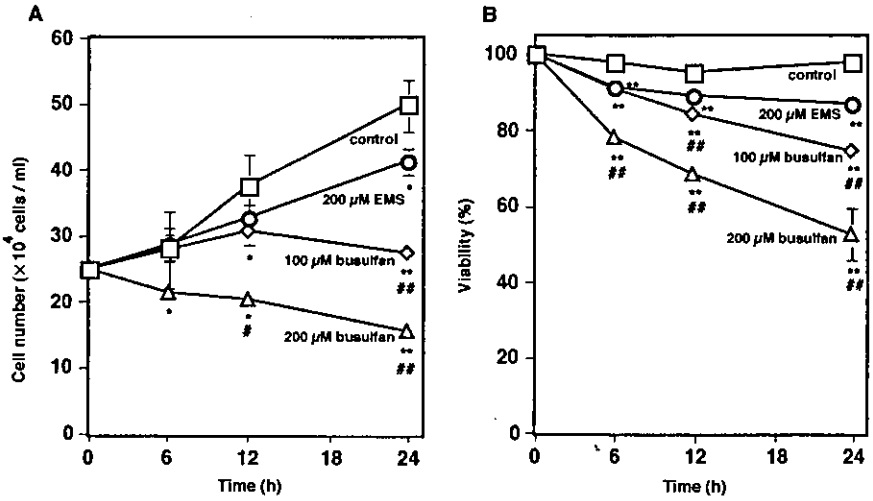

Fig. 1. Effects of busulfan and EMS on the growth and viability of cultured cells. HL-60 cells (2.5×10^5 cells/ml) were incubated with no drug (square), 100 μ*M* busulfan (diamond), 200 μ*M* busulfan (triangle) or 200 μ*M* EMS (circle) at 37°C. Cell number (A) and viability (B) were determined by trypan blue exclusion and counting in a hemocytometer. Values represent means±SD of four independent experiments. * $P<0.05$, and ** $P<0.01$ statistically significant difference compared with the control; # $P<0.05$, and ## $P<0.01$ between busulfan and EMS.

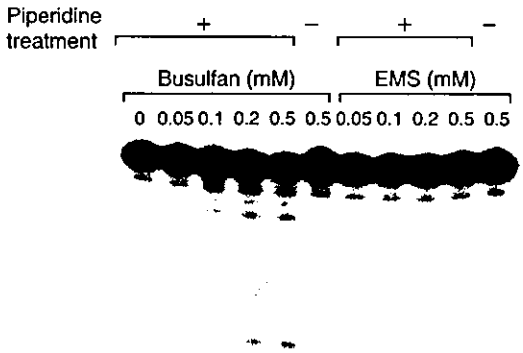

Fig. 2. Autoradiogram of ^{32}P-labeled DNA fragments incubated with busulfan and EMS. The reaction mixture (in a 1.5 ml Eppendorf microtube) contained busulfan or EMS, ^{32}P-end-labeled 156-bp DNA fragments, and calf thymus DNA (2 μ*M*/base) in 200 μl of 10 m*M* sodium phosphate buffer (pH 6.4) containing 5 μ*M* DTPA. After incubation for 1.5 h at 37°C, the DNA fragments were treated with 1 *M* piperidine for 20 min at 90°C. The DNA fragments were then subjected to electrophoresis on an 8 *M* urea/8% polyacrylamide gel and visualized by autoradiography.

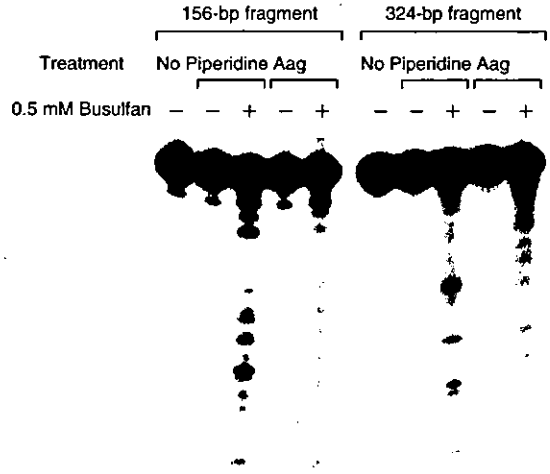

Fig. 3. Effects of piperidine and Aag treatment on DNA damage induced by busulfan. The reaction mixture contained 0.5 m*M* busulfan, 324-bp ^{32}P-5′-end-labeled DNA fragments and calf thymus DNA (2 μ*M*/base) in 200 μl of 10 m*M* sodium phosphate buffer (pH 6.4) containing 5 μ*M* DTPA. Reaction mixtures were incubated for 1.5 h at 37°C. After incubation, the DNA fragments were treated with 1 *M* piperidine for 20 min at 90°C or 3 units of Aag for 24 h at 37°C. The treated DNA fragments were analyzed as described in Fig. 2 legend.

phosphate buffer (pH 6.4) containing 5 μ*M* DTPA. After incubation for 1.5 h at 37°C, the DNA fragments were treated with 1 *M* piperidine for 20 min at 90°C[14] or 3 units of Aag in the reaction buffer (10 m*M* HEPES-KOH (pH 7.4), 100 m*M* KCl, 1 m*M* EDTA, 1 m*M* EGTA and 0.1 m*M* DTT) for 24 h at 37°C. After ethanol precipitation, the DNA fragments were electrophoresed and the autoradiogram was obtained by exposing X-ray film to the gel as described previously.[14]

The preferred binding sites of busulfan were determined by direct comparison of the positions of the oligonucleotides with those of oligonucleotides produced by the chemical reactions of the Maxam-Gilbert procedure[15] using a DNA-sequencing system (LKB 2010 Macrophor, Pharmacia Biotech, Uppsala, Sweden). The relative amounts of oligonucleotides from the treated DNA fragments were measured with a laser densitometer (LKB 2222 UltroScan XL, Pharmacia Biotech).

TOF-MS analysis of DNA adducts formed by busulfan. Reaction mixtures containing 0.5 m*M* busulfan and 0.1 m*M* self-complementary 10-base oligonucleotide (5′-GCTGATCAGC-3′, Sawady Technology Co., Tokyo) in 10 m*M* sodium phosphate buffer (pH 6.4) containing 5 μ*M* DTPA were incubated for 24 h at 37°C. After incubation, the reaction mixture and 50 mg/ml matrix solution (3-hydroxypicolinic acid:citric acid=8:1) were loaded onto a sample plate. The molecular weight of DNA adducts was analyzed by using TOF-MS, which was performed on a Voyager B-RP (PerSeptive Biosystems, Framingham, MA) equipped with a nitrogen laser (337 nm, 3 ns pulse).

Results

Growth-inhibitory and cytotoxic effects of busulfan and EMS. Fig. 1 shows the effects of busulfan and EMS on the growth and viability of human HL-60 cells. Since busulfan is a bifunctional agent, a 2-fold larger amount of EMS is considered to have the same number of reaction sites as those of busulfan. Busulfan

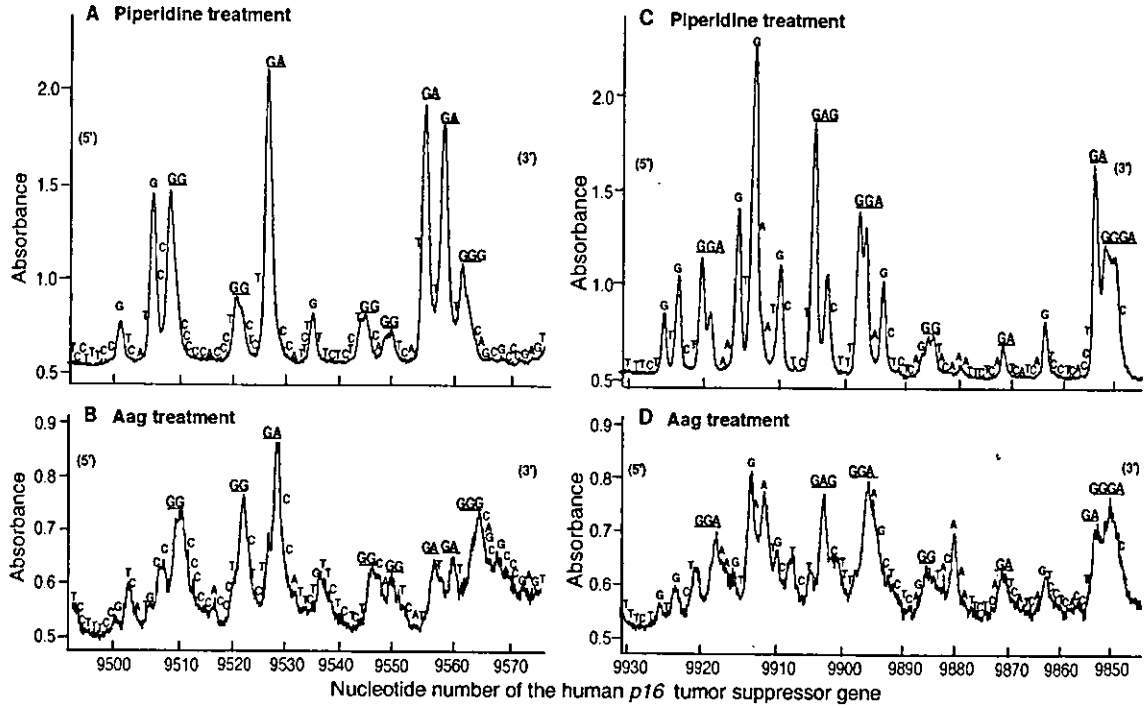

Fig. 4. Site specificity of DNA damage induced by busulfan. Reaction mixtures contained 0.5 m*M* busulfan, ^{32}P-5'-end-labeled 324-bp (A, B) or 156-bp (C, D) fragment and calf thymus DNA (2 μ*M*/base) in 200 μl of 10 m*M* sodium phosphate buffer (pH 6.4) containing 5 μ*M* DTPA. Reaction mixtures were incubated for 30 min at 37°C, followed by piperidine (A, C) or Aag (B, D) treatment. The treated DNA fragments were analyzed as described in Fig. 2 legend. The relative quantities of oligonucleotides were measured by scanning the autoradiogram (LKB 2222 UltroScan XL, Pharmacia Biotech).

showed a significant inhibitory effect on cell growth at 100 μ*M* ($P<0.05$) compared with the control after the 12 h treatment, whereas the cells grew in the presence of 200 μ*M* EMS (Fig. 1A). Furthermore, 200 μ*M* busulfan significantly decreased the cell number after the 6 h treatment ($p<0.05$, Fig. 1A). Both 100 μ*M* and 200 μ*M* busulfan significantly reduced the cell viability compared with 200 μ*M* EMS after the 12 h and 6 h treatment, respectively ($P<0.01$, Fig. 1B).

Damage to ^{32}P-labeled DNA fragments induced by busulfan and EMS. Fig. 2 shows the autoradiogram of DNA fragments treated with busulfan and EMS. Oligonucleotides were detected on the autoradiogram as a result of DNA damage. The intensity of DNA damage induced by busulfan increased with increasing concentration. No DNA damage was observed when the DNA fragments were not treated with piperidine or Aag, suggesting that busulfan causes only base modification (Figs. 2 and 3). EMS induced little DNA damage (Fig. 2). The pattern of Aag-sensitive lesions was different from that of piperidine-labile lesions (Fig. 3).

Site specificity of DNA damage induced by busulfan. An autoradiogram was obtained and scanned with a laser densitometer to measure the relative intensity of DNA damage in the human *p16* tumor suppressor gene (Fig. 4). DNA was frequently damaged at guanine residues, especially at 5'-GA-3' and 5'-GG-3' sequences, with piperidine treatment. With Aag treatment, DNA damage occurred at guanine and adenine residues mainly at 5'-GA-3' and, to a lesser extent, 5'-GG-3' sequences.

Mass spectrum of oligonucleotide treated with busulfan. We performed mass spectrometry to detect cross-linking by busulfan using a self-complementary oligonucleotide (5'-GCTGATCAGC-3'/3'-CGACTAGTCG-5'). Fig. 5 shows the mass spectrum of the oligonucleotide treated with busulfan. The signal at m/z=3029 was assigned to the intact oligonucleotide. It can be explained by assuming that busulfan reacted with the double-

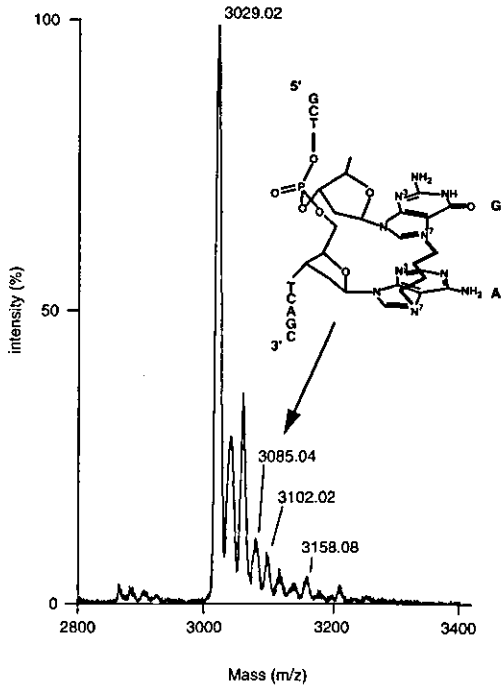

Fig. 5. Mass spectrum of the oligonucleotide treated with busulfan. Reaction mixtures containing 0.5 m*M* busulfan and 0.1 m*M* 10-base oligonucleotide (5'-GCTGATCAGC-3') were incubated at 37°C for 24 h. After the incubation, the reaction mixture and 50 mg/ml matrix solution (3-hydroxypicolinic acid:citric acid=8:1) were loaded onto a sample plate. The mass spectrum was obtained from 50 laser shots. TOF-MS analysis was performed on a Voyager B-RP (PerSeptive Biosystems) equipped with a nitrogen laser (337 nm, 3 ns pulse). The proposed structure of G-A intrastrand cross-link of busulfan is shown.

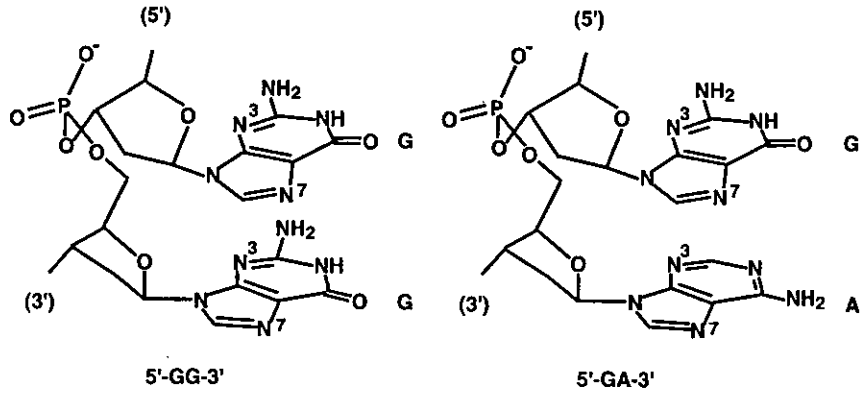

Fig. 6. Chemical structures of 5′-GG-3′ and 5′-GA-3′ sequences.

stranded oligonucleotide, and then the oligonucleotide was denatured in the acidic matrix solution. The signal at m/z=3085, was assigned to the cross-linking of $(CH_2)_4$ to the oligonucleotide. The signal at m/z=3102 showed the formation of a $(CH_2)_4OH$ adduct, while that at m/z=3158 showed the addition of $(CH_2)_4$ and $(CH_2)_4OH$ to the oligonucleotide. These results suggest that busulfan produced an intrastrand cross-link in DNA or mono-alkylation at purine bases.

Discussion

In the present study, we compared the cytotoxic activity and DNA-damaging ability of bifunctional busulfan with those of monofunctional EMS. Busulfan showed a significant inhibitory effect on cell growth and reduced the viability compared with EMS. Busulfan dose-dependently induced damage to isolated DNA, whereas EMS induced little DNA damage. These results indicate that busulfan has higher affinity for DNA than does EMS, and that DNA damage plays an important role in cytotoxicity. Furthermore, busulfan showed a significant cytotoxic effect compared with a 2-fold larger amount of EMS, suggesting that a mechanism other than DNA mono-alkylation contributes to the more potent cytotoxic effect of busulfan. The mechanism can be explained by the observation that busulfan formed cross-links in DNA. This finding seems to favor the idea that cross-link lesions may be more difficult to repair than mono-alkylation.[16] Glufosfamide, a bifunctional alkylating agent, also induced cytotoxic lesions mainly by cross-linking, as shown by a comparison of isogenic cell lines deficient and proficient in cross-link repair.[17]

A previous study has shown that the alkylation of DNA induced by nitrogen mustard gave four principal products, derived from mono-alkylation of guanine at N7 and adenine at N3 and from cross-linking of G-G or G-A at these positions.[18] As for busulfan, interaction with guanosine resulted in the formation of 1,4-di(7-guanosinyl)butane, suggesting that busulfan forms a G-G cross-link.[10] Since busulfan, with a maximum extended configuration of 6.0 Å, would be unable to span the distance between N7 atoms of adjacent guanosines on opposite DNA strands (a narrow groove distance of 8.0 Å in B form DNA),[10,19] busulfan is likely to form intrastrand cross-links. The chemical structures of the 5′-GG-3′ and 5′-GA-3′ sequences are shown in Fig. 6. It remains uncertain whether busulfan produces DNA alkylation at adenine residues. Notably, DNA-sequencing experiments using Aag protein and piperidine suggest that busulfan induces DNA alkylation mainly at 5′-GA-3′ and, to a lesser extent, 5′-GG-3′ sequences. Aag catalyzes the excision of alkylated guanine and adenine.[20–25] The mass spectrum of the busulfan-treated oligonucleotide containing the GA sequence suggests that $(CH_2)_4$ is bound at both ends to the oligonucleotide to form an intrastrand cross-link and that $(CH_2)_4OH$ is bound to form a mono-adduct. These results provide the first evidence for DNA intrastrand cross-linking of busulfan at the 5′-GA-3′ sequence.

It is known that the N7 and O6 positions of guanine and the N3 position of adenine are the alkylation sites for most chemotherapeutic alkylating agents.[5,6] Westerhof *et al.* reported that O6-guanine alkylation is not important for the chemotherapeutic effects of busulfan, because overexpression of O6-alkylguanine-DNA-alkyltransferase, which removes O6-alkylated guanine, had no effect on the cytotoxicity.[26] In the 5′-GA-3′ sequence, the distance between N7 of guanine and N3 of adjacent adenine exceeds the length of busulfan in duplex DNA. Therefore, the possibility of binding in this manner can be excluded. Alternatively, possible sites of DNA intrastrand cross-linking are the N7 positions of guanine and adenine or the N3 positions of guanine and adenine. One of the busulfan analogues, hepsulfam (1,7-heptanediol disulfamate), was reported to be mainly bound to the N7 position of guanine but not the N3 position of adenine.[27] It was reported that dimethyl sulfate formed a variety of alkylated bases, including N7-methylguanine, N3-methyladenine and N7-methyladenine, with DNA.[28] These reports support the idea that busulfan is likely to bind to the N7 positions of guanine and adenine rather than the N3 positions to form DNA intrastrand cross-links. We have previously reported that DNA alkylation induces apoptosis through the generation of H_2O_2.[29] Therefore, an apoptotic pathway via DNA alkylation at the N7 positions of guanine and adenine may be responsible for the cytotoxic effect of busulfan. In conclusion, the formation of DNA intrastrand cross-links is considered to be the mechanism of the strong cytotoxicity induced by busulfan.

1. Kohn KW. Beyond DNA cross-linking: history and prospects of DNA-targeted cancer treatment-fifteenth Bruce F. Cain Memorial Award Lecture. *Cancer Res* 1996; 56: 5533–46.
2. Hurley LH. DNA and its associated processes as targets for cancer therapy. *Nat Rev Cancer* 2002; 2: 188–200.
3. Newbold RF, Warren W, Medcalf AS, Amos J. Mutagenicity of carcinogenic methylating agents is associated with a specific DNA modification. *Nature* 1980; 283: 596–9.
4. Lawley PD, Phillips DH. DNA adducts from chemotherapeutic agents. *Mutat Res* 1996; 355: 13–40.
5. Brookes P, Lawley PD. Reaction of mustard gas with nucleic acids *in vitro* and *in vivo*. *Biochem J* 1960; 77: 478–84.
6. Kohn KW, Hartley JA, Mattes WB. Mechanisms of DNA sequence selective alkylation of guanine-N7 positions by nitrogen mustards. *Nucleic Acids Res* 1987; 15: 10531–49.
7. Buggia I, Locatelli F, Regazzi MB, Zecca, M. Busulfan. *Ann Pharmacother* 1994; 28: 1055–62.
8. Westerhof GR, Ploemacher RE, Boudewijn A, Blokland I, Dillingh JH,

McGown AT, Hadfield JA, Dawson MJ, Down JD. Comparison of different busulfan analogues for depletion of hematopoietic stem cells and promotion of donor-type chimerism in murine bone marrow transplant recipients. *Cancer Res* 2000; **60**: 5470–8.
9. Brookes P, Lawley PD. The reactions of mono- and difunctional alkylating agents with nucleic acids. *Biochem J* 1960; **80**: 496–8.
10. Tong WP, Ludlum DB. Crosslinking of DNA by busulfan. Formation of diguanyl derivatives. *Biochim Biophys Acta* 1980; **608**: 174–81.
11. Ponti M, Souhami RL, Fox BW, Hartley JA. DNA interstrand crosslinking and sequence selectivity of dimethanesulphonates. *Br J Cancer* 1991; **63**: 743–7.
12. Serrano M, Hannon GJ, Beach DA. A new regulatory motif in cell-cycle control causing specific inhibition of cyclin D/CDK4. *Nature* 1993; **366**: 704–7.
13. Oikawa S, Murakami K, Kawanishi S. Oxidative damage to cellular and isolated DNA by homocysteine: implications for carcinogenesis. *Oncogene* 2003; **22**: 3530–8.
14. Oikawa S, Kawanishi S. Detection of DNA damage and analysis of its site-specificity. In: Taniguchi N, Gutteridge JMC, editors. Experimental protocols for reactive oxygen and nitrogen species. New York: Oxford University Press; 2000. p. 229–35.
15. Maxam AM, Gilbert W. Sequencing end-labeled DNA with base-specific chemical cleavages. *Methods Enzymol* 1980; **65**: 499–560.
16. Hemminki K, Ludlum DB. Covalent modification of DNA by antineoplastic agents. *J Natl Cancer Inst* 1984; **73**: 1021–8.
17. Seker H, Bertram B, Burkle A, Kaina B, Pohl J, Koepsell H, Wiesser M. Mechanistic aspects of the cytotoxic activity of glufosfamide, a new tumour therapeutic agent. *Br J Cancer* 2000; **82**: 629–34.
18. Osborne MR, Wilman DE, Lawley PD. Alkylation of DNA by the nitrogen mustard bis(2-chloroethyl)methylamine. *Chem Res Toxicol* 1995; **8**: 316–20.
19. Bedford P, Fox BW. DNA-DNA interstrand crosslinking by dimethanesulphonic acid esters. Correlation with cytotoxicity and antitumour activity in the Yoshida lymphosarcoma model and relationship to chain length. *Biochem Pharmacol* 1983; **32**: 2297–301.
20. Dosanjh MK, Roy R, Mitra S, Singer B. 1,N6-Ethenoadenine is preferred over 3-methyladenine as substrate by a cloned human N-methylpurine-DNA glycosylase (3-methyladenine-DNA glycosylase). *Biochemistry* 1994; **33**: 1624–8.
21. Mattes WB, Lee CS, Laval J, O'Connor TR. Excision of DNA adducts of nitrogen mustards by bacterial and mammalian 3-methyladenine-DNA glycosylases. *Carcinogenesis* 1996; **17**: 643–8.
22. Roy R, Kennel SJ, Mitra S. Distinct substrate preference of human and mouse N-methylpurine-DNA glycosylases. *Carcinogenesis* 1996; **17**: 2177–82.
23. Saparbaev M, Laval J. Excision of hypoxanthine from DNA containing dIMP residues by the *Escherichia coli*, yeast, rat, and human alkylpurine DNA glycosylases. *Proc Natl Acad Sci USA* 1994; **91**: 5873–7.
24. Saparbaev M, Kleibl K, Laval J. *Escherichia coli*, *Saccharomyces cerevisiae*, rat and human 3-methyladenine DNA glycosylases repair 1,N6-ethenoadenine when present in DNA. *Nucleic Acids Res* 1995; **23**: 3750–5.
25. Bouziane M, Miao F, Ye N, Holmquist G, Chyzak G, O'Connor TR. Repair of DNA alkylation damage. *Acta Biochim Pol* 1998; **45**: 191–202.
26. Westerhof GR, Down JD, Blokland I, Wood M, Boudewijn A, Watson AJ, McGown AT, Ploemacher RE, Margison GP. O6-Benzylguanine potentiates BCNU but not busulfan toxicity in hematopoietic stem cells. *Exp Hematol* 2001; **29**: 633–8.
27. Je KH, Son JK, O'Connor TR, Lee CS. Hepsulfam induced DNA adducts and its excision repair by bacterial and mammalian 3-methyladenine DNA glycosylases. *Mol Cells* 1998; **8**: 691–7.
28. Shiner AC, Newbold RF, Cooper CS. Morphological transformation of immortalized hamster dermal fibroblasts following treatment with simple alkylating carcinogens. *Carcinogenesis* 1988; **9**: 1701–9.
29. Tada-Oikawa S, Oikawa S, Kawanishi M, Yamada M, Kawanishi S. Generation of hydrogen peroxide precedes loss of mitochondrial membrane potential during DNA alkylation-induced apoptosis. *FEBS Lett* 1999; **442**: 65–9.

Available online at www.sciencedirect.com
SCIENCE DIRECT®
Biochemical and Biophysical Research Communications 316 (2004) 123–128
BBRC
www.elsevier.com/locate/ybbrc

Oxidative DNA damage induced by nitrotyrosine, a biomarker of inflammation☆

Mariko Murata and Shosuke Kawanishi*

Department of Environmental and Molecular Medicine, Mie University School of Medicine, Edobashi, Tsu, Mie 514-8507, Japan

Received 19 December 2003

Abstract

Inflammation has been postulated as a risk factor for several cancers. 3-Nitrotyrosine is a biochemical marker for inflammation. We investigated the ability of nitrotyrosine and nitrotyrosine-containing peptides (nitroY-peptide) to induce DNA damage by the experiments using ^{32}P-labeled DNA fragments obtained from the human *p53* tumor suppressor gene and an HPLC-electrochemical detector. Nitrotyrosine and nitroY-peptide caused Cu(II)-dependent DNA damage in the presence of P450 reductase, which is considered to yield nitroreduction. Catalase inhibited DNA damage, suggesting the involvement of H_2O_2. Nitrotyrosine and nitroY-peptide increased 8-oxo-7,8-dihydro-2′-deoxyguanosine (8-oxodG) formation, an indicator of oxidative DNA damage. Nitrotyrosine-containing peptides of histone induced 8-oxodG formation more efficiently than free nitrotyrosine. We propose the possibility that nitrotyrosine-induced H_2O_2 formation and DNA damage contribute to inflammation-associated carcinogenesis.

Keywords: Nitrotyrosine; Oxidative DNA damage; P450 reductase; Copper; Hydrogen peroxide; Inflammation; Carcinogenesis

Inflammation has been postulated as a risk factor for several cancers [1–5]. Inflammation and infection activate a variety of inflammatory cells, which produce nitric oxide (NO) and superoxide ($O_2^{\cdot-}$), yielding peroxynitrite ($ONOO^-$), and other types of reactive nitrogen species (RNS) [6,7]. The reaction of RNS with protein-bound tyrosine residues causes nitrotyrosine formation in inflammatory and infected tissues. Many studies revealed the presence of 3-nitrotyrosine in human tissues and fluids due to inflammation and infectious diseases [8–11]. Nitrotyrosine serves as a biochemical marker for inflammation. Increases of protein tyrosine nitration were observed in cancer sites [12,13]. Interestingly, a recent study has suggested that histones are the most prominent nitrated proteins in the Mutatec tumor tissue exposed to NO [14]. Irie et al. [15] have demonstrated that histone is a substrate for "denitrase" that removes the nitro group of nitrotyrosine in proteins. The existence of a repair mechanism for nitrated tyrosine in histone has led us to an idea that nitrotyrosine may have deleterious effects on biological system. There arises a possibility that nitrotyrosine can be involved in DNA damage, which may participate in inflammation-associated carcinogenesis.

We investigated the ability of nitrotyrosine and nitrotyrosine-containing peptides of histone to induce DNA damage using ^{32}P-labeled DNA fragments obtained from the human *p53* and *p16* tumor suppressor genes. We also analyzed 8-oxo-7,8-dihydro-2′-deoxyguanosine (8-oxodG) formation in calf thymus DNA with an electrochemical detector coupled to an HPLC (HPLC-ECD), as an indicator of oxidative DNA damage.

Materials and methods

Materials. Restriction enzymes (*Eco*RI, *Mro*I, and *Apa*I) and calf intestine phosphatase were purchased from Boehringer–Mannheim (Germany). Restriction enzymes (*Hin*dIII and *Ava*I) and T_4 polynucleotide

☆ *Abbreviations:* nitroY-peptide, nitrotyrosine-containing peptide; RNS, reactive nitrogen species; 8-oxodG, 8-oxo-7,8-dihydro-2′-deoxyguanosine (and also known as 8-hydroxy-2′-deoxyguanosine); DTPA, diethylenetriamine-*N*,*N*,*N*′,*N*″,*N*″-pentaacetic acid; HPLC-ECD, high performance liquid chromatography coupled with an electrochemical detector; NADPH, β-nicotinamide adenine dinucleotide phosphate (reduced form); P450 reductase, NADPH-cytochrome P450 reductase; SOD, superoxide dismutase.

* Corresponding author. Fax: +81-59-231-5011.
E-mail address: kawanisi@doc.medic.mie-u.ac.jp (S. Kawanishi).

0006-291X/$ - see front matter © 2004 Elsevier Inc. All rights reserved.
doi:10.1016/j.bbrc.2004.02.022

kinase were purchased from New England Biolabs. [γ-^{32}P]ATP (222 TBq/mmol) was from New England Nuclear. Superoxide dismutase (SOD, 3000 U/mg from bovine erythrocytes) and catalase (45,000 U/mg from bovine liver) were from Sigma Chemical. Nitrotyrosine-containing peptides (nitroY-peptide) were supplied by Sawady Technology (Tokyo, Japan; nitroY1-peptide) and Nihon Sigma Genosys Biotechnologies (Hokkaido, Japan; nitroY3-peptide). The amino acid sequences of nitrated tyrosine residue on histone were from reference [14] that identified them in tumor tissue by mass spectrometry as follows; nitroY1-peptide; nitroY-R-P-G-T-V-A-L-R and nitroY3-peptide; E-S-nitroY-S-V-nitroY-V-nitroY-K. NADPH, NADP$^+$, acrylamide, bisacrylamide, and piperidine were obtained from Wako Pure Chemical Industries (Osaka, Japan). NADPH-cytochrome P450 reductase (P450 reductase) from rat microsome was a kind gift from Dr. Y. Kumagai (Tsukuba University). Ethanol and $CuCl_2$ were from Nakalai Tesque (Kyoto, Japan). Nuclease P_1 was from Yamasa Shoyu (Chiba, Japan). Bathocuproinedisulfonic acid was from Dojin Chemicals (Kumamoto, Japan).

Preparation of ^{32}P-5′-end-labeled DNA fragments. DNA fragments obtained from the human *p53* tumor suppressor gene [16] containing exons were prepared, as described previously [17]. The 5′-end-labeled 650-bp fragment (*Hin*dIII*13972–*Eco*RI*14621) was obtained by dephosphorylation with calf intestine phosphatase and rephosphorylation with [γ-^{32}P]ATP and T_4 polynucleotide kinase (*, ^{32}P-labeled). The 650-bp fragment was further digested with *Apa*I to obtain a singly labeled 443-bp fragment (*Apa*I 14179–*Eco*RI*14621) and a 211-bp fragment (*Hin*dIII*13972–*Apa*I 14182). DNA fragment was also obtained from the human *p16* tumor suppressor gene [18]. The 5′ end-labeled 490-bp fragment (*Eco*RI*5841–*Eco*RI*6330) containing exon 1 of the human *p16* tumor suppressor gene was obtained by pGEM-T Easy Vector (Promega). The 490-bp fragment was further digested with *Mro*I to obtain a singly labeled 328-bp fragment (*Eco*RI*5841–*Mro*I 6168) and a 158-bp fragment (*Mro*I 6173–*Eco*RI*6330) as described previously [19].

Detection of DNA damage by nitrotyrosine. The standard reaction mixtures (in a microtube; 1.5 mL; Eppendorf) containing nitrotyrosine, 100 μM NADPH, and P450 reductase in 20 mM potassium phosphate buffer (pH 7.4) were pre-incubated at 25 °C for 30 min. After pre-incubation, ^{32}P-5′-end-labeled DNA fragments, calf thymus DNA (20 μM/base), and 20 μM $CuCl_2$ were added to the mixtures (total 200 μL), followed by the incubation at 37 °C for 1 h. Then, the DNA fragments were treated in 10% (v/v) piperidine at 90 °C for 20 min, or treated with 6 U Fpg protein in 21 μL of reaction buffer (10 mM Hepes–KOH (pH 7.4), 100 mM KCl, 10 mM EDTA, and 0.1 mg/ml BSA) at 37 °C for 2 h. The treated DNA was electrophoresed on an 8% polyacrylamide/8 M urea gel. The autoradiogram was obtained by exposing X-ray film to the gel [19].

The preferred cleavage sites were determined by direct comparison of the positions of the oligonucleotides with those produced by the chemical reactions of the Maxam–Gilbert procedure [20] using a DNA-sequencing system (LKB 2010 Macrophor). The relative amounts of oligonucleotides from the treated DNA fragments were measured with a laser densitometer (LKB 2222 UltroScan XL).

Analysis of 8-oxodG formation in calf thymus DNA by nitrotyrosine. The standard reaction mixture (in a microtube; 1.5 mL; Eppendorf) containing nitrotyrosine, 100 μM NADPH, and P450 reductase in 20 mM potassium phosphate buffer (pH 7.4) were pre-incubated at 25 °C for 30 min. After pre-incubation, calf thymus DNA (100 μM/base) and 20 μM $CuCl_2$ were added, and then incubated at 37 °C for 1 h. After ethanol precipitation, DNA was digested to the nucleosides with nuclease P_1 and calf intestine phosphatase, and analyzed by an HPLC-ECD, as described previously [21].

Measurement of NADP$^+$ amount. The standard reaction mixtures (in a microtube; 1.5 mL; Eppendorf) containing nitrotyrosine, 100 μM NADPH and P450 reductase in 20 mM potassium phosphate buffer (pH 7.4) were pre-incubated at 25 °C for 30 min, followed by incubation at 37 °C for 1 h. NADP$^+$ amount was analyzed by HPLC with a Shimadzu photodiode array UV detector (SPD-M10A, Kyoto, Japan) at 260 nm with Wako Pure Chemical ODS (46 mm × 150 mm) in mobile phase containing 2% methanol and 100 mM potassium phosphate buffer (pH 6) at flow rate 1 mL/min.

Results

Damage to ^{32}P-labeled DNA fragments by nitrotyrosine in the presence of P450 reductase, NADPH, and Cu(II)

Free nitrotyrosine and nitrotyrosine-peptides of histone caused Cu(II)-mediated DNA damage when

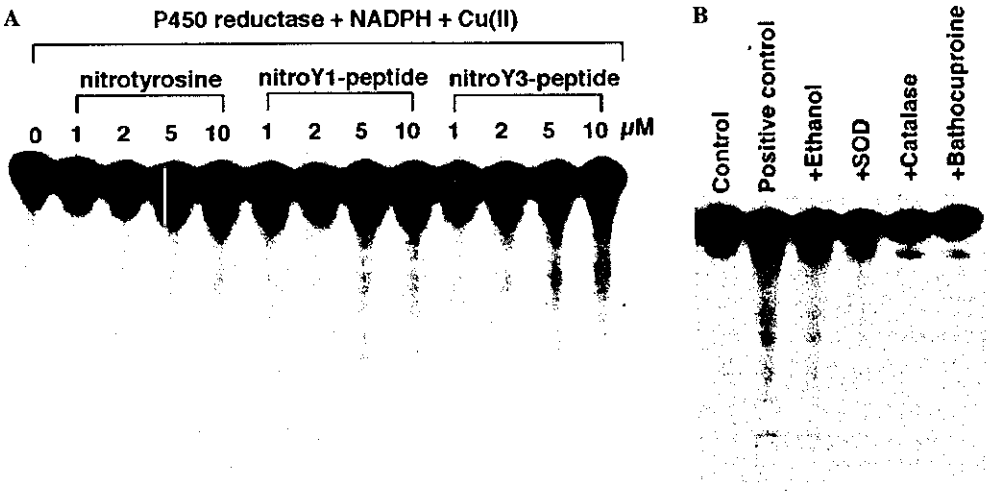

Fig. 1. Autoradiograms of ^{32}P-labeled DNA fragments incubated with free nitrotyrosine and nitroY-peptides in the presence of P450 reductase, NADPH, and Cu(II). (A) The reaction mixtures containing indicated concentrations of nitrotyrosine or nitroY-peptide, 100 μM NADPH, and 2.1 μg/mL P450 reductase in 20 mM potassium phosphate buffer (pH 7.4) were pre-incubated at 25 °C for 30 min. After pre-incubation, ^{32}P-5′-end-labeled 158-bp DNA fragments, calf thymus DNA (20 μM/base), and 20 μM $CuCl_2$ were added to the mixtures (total 200 μL), followed by the incubation at 37 °C for 1 h. (B) Scavengers were added after pre-incubation of 10 μM nitroY3-peptide as follows: 5% (v/v) ethanol; 30 U SOD; 30 U catalase; 50 μM bathocuproine. After the incubation, the DNA fragments were treated with hot piperidine and electrophoresed on an 8% polyacrylamide/8 M urea gel. The autoradiogram was obtained by exposing X-ray film to the gel.

they were treated with P450 reductase (Fig. 1A). Without P450 reductase, free nitrotyrosine and nitroY-peptides caused no DNA damage even in the presence of Cu(II) (data not shown). In the absence of Cu(II), DNA damage was not observed. Free nitrotyrosine induced slight DNA damage. NitroY-peptides damaged DNA more efficiently than free nitrotyrosine. The peptide containing three nitrotyrosine residues (nitroY3-peptide) induced DNA damage stronger than that containing one nitrotyrosine (nitroY1-peptide). The amount of oligonucleotides was increased by piperidine treatment, suggesting the involvement of base modification/liberation (data not shown).

Effects of scavengers and bathocuproine on DNA damage induced by nitrotyrosine

Fig. 1B shows the effects of scavengers and bathocuproine, a Cu(I)-specific chelator, on DNA damage induced by P450 reductase-treated nitroY3-peptide in the presence of Cu(II). Catalase and bathocuproine inhibited DNA damage, suggesting the involvement of hydrogen peroxide (H_2O_2) and Cu(I). Ethanol, a typical free hydroxyl radical (·OH) scavenger, did not attenuate DNA damage. SOD partly inhibited DNA damage. Similar results were obtained with nitroY1-peptide (data not shown).

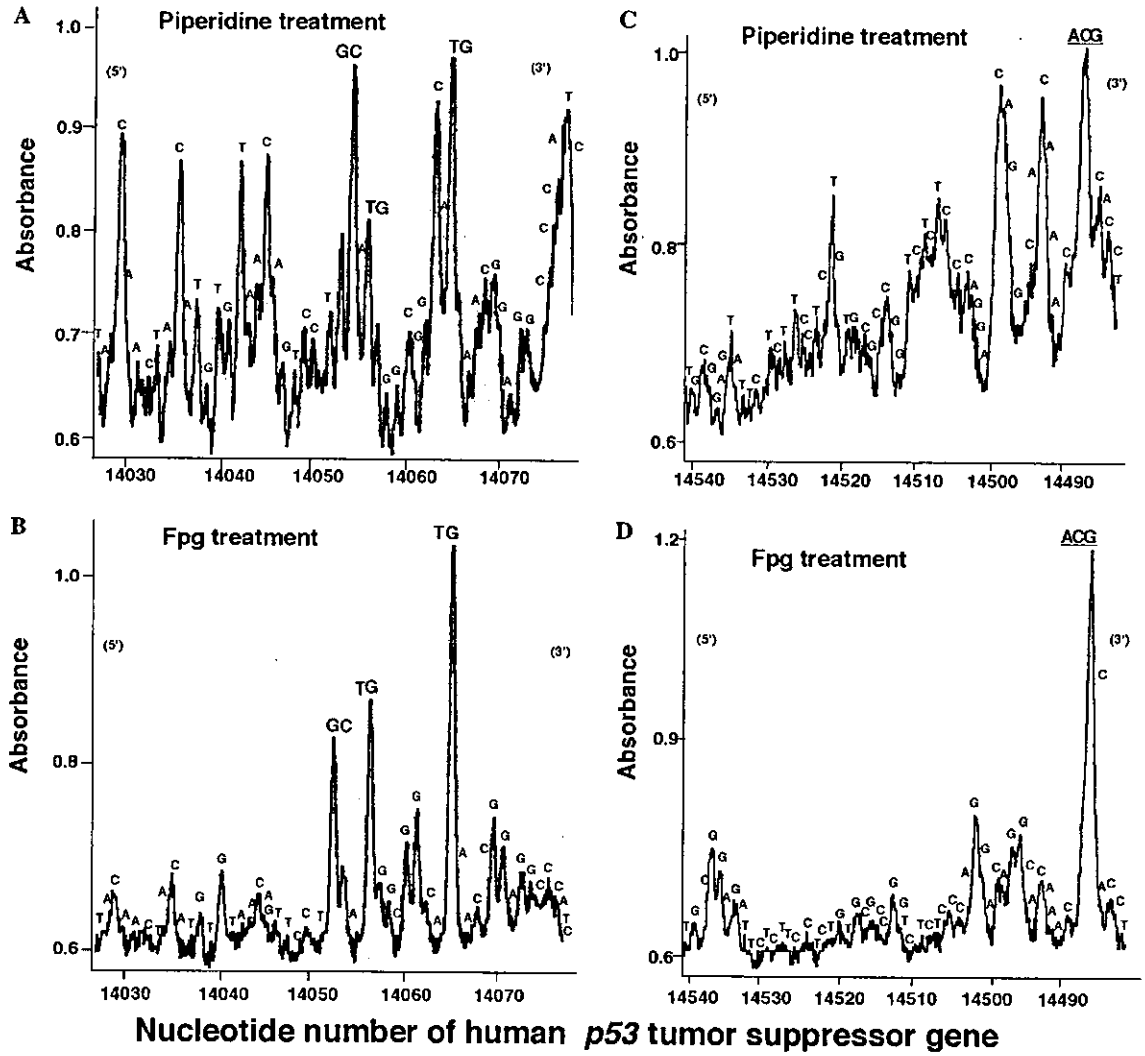

Fig. 2. Site specificity of Cu(II)-mediated DNA cleavage induced by nitroY3-peptide in the presence of P450 reductase. The reaction mixtures containing 10 μM nitroY3-peptide, 100 μM NADPH, and 2.1 μg/mL P450 reductase in 20 mM potassium phosphate buffer (pH 7.4) were pre-incubated at 25 °C for 30 min. After pre-incubation, ^{32}P-5′-end-labeled 211-bp (A,B) or 443-bp (C,D) DNA fragments, calf thymus DNA (20 μM/base), and 20 μM $CuCl_2$ were added to the mixtures. Reaction mixtures were incubated at 37 °C for 1 h, followed by hot piperidine (A,C) and Fpg treatment (B,D). DNA fragments were electrophoresed on an 8% polyacrylamide/8 M urea gel using a DNA-sequencing system and the autoradiogram was obtained by exposing X-ray film to the gel. The relative amounts of oligonucleotide were measured by scanning the autoradiogram with a laser densitometer (LKB 2222 UltroScan XL). The horizontal axis shows the nucleotide number of the human *p53* tumor suppressor gene and underscoring shows the complementary sequence to codon 273 (nucleotide numbers 14486–14488).

Site specificity of DNA cleavage by nitrotyrosine

An autoradiogram was obtained and scanned with a laser densitometer to measure relative intensity of DNA cleavage in the human *p53* tumor suppressor gene (Fig. 2). P450 reductase-treated nitroY-peptide induced piperidine-labile sites relatively at thymine and cytosine residues in the presence of Cu(II) (Figs. 2A and C). With Fpg treatment, DNA cleavage occurred mainly at guanine residues (Figs. 2B and D). Collectively, damage at neighboring guanine and pyrimidine residues such as 5′-TG-3′ and 5′-GC-3′ sites was observed (Figs. 2A and B), suggesting that double-base lesion occurred. NitroY-peptides caused piperidine-labile and Fpg-sensitive lesions at CG in the 5′-ACG-3′ sequence, a well-known hotspot of the *p53* gene [22] (Figs. 2C and D).

Formation of 8-oxodG in calf thymus DNA by nitrotyrosine

Using an HPLC-ECD, we measured 8-oxodG content in calf thymus DNA treated with nitrotyrosine after P450 reductase treatment (Fig. 3). NitroY3-peptide increased the amount of 8-oxodG up to 2 μM and then decreased gradually. Significant increases ($p < 0.01$) were observed in all conditions treated with 1 μM and higher concentrations of nitroY3-peptide. NitroY1-peptide induced the increase of

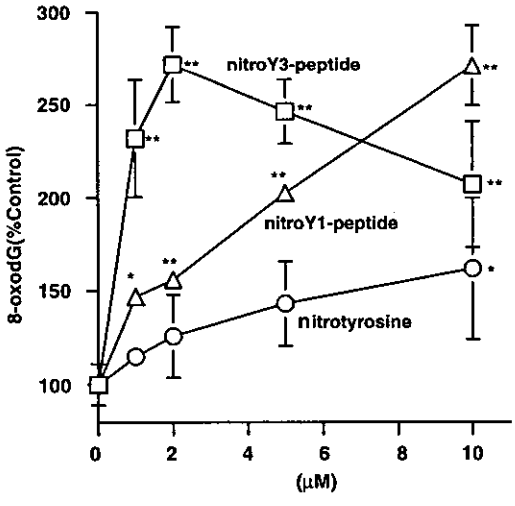

Fig. 3. Cu(II)-mediated formation of 8-oxodG in calf thymus DNA by nitrotyrosine and nitroY-peptides in the presence of P450 reductase. The reaction mixtures containing nitrotyrosine or nitroY-peptides, 100 μM NADPH, and 2.1 μg/mL P450 reductase in 20 mM potassium phosphate buffer (pH 7.4) were pre-incubated at 25 °C for 30 min. After pre-incubation, DNA fragments (100 μM/base) from calf thymus and 20 μM $CuCl_2$ were added and then incubated at 37 °C for 1 h. After ethanol precipitation, DNA was enzymatically digested to the nucleosides and analyzed by an HPLC-ECD. Results are expressed as means (control; 100%) and SEM of values obtained from three independent experiments. Asterisks indicate significant difference compared with control by Student's *t* test (*$p < 0.05$, **$p < 0.01$).

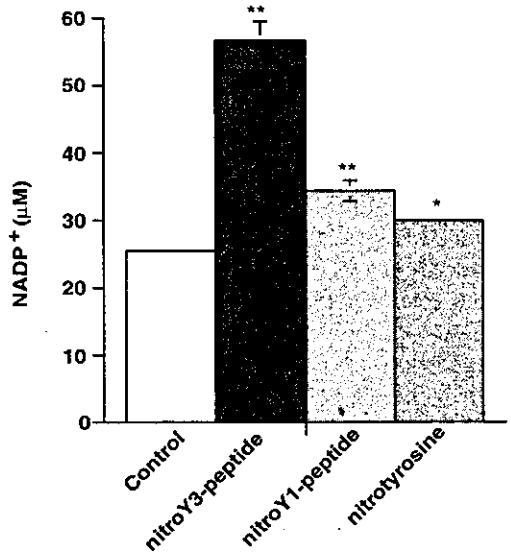

Fig. 4. Production of $NADP^+$ through reaction of nitrotyrosines and P450 reductase. The reaction mixtures containing 10 μM nitrotyrosine or nitroY-peptides, 100 μM NADPH, and 2.1 μg/mL P450 reductase in 20 mM potassium phosphate buffer (pH 7.4) were pre-incubated at 25 °C for 30 min, followed by incubation at 37 °C for 1 h. $NADP^+$ amount was analyzed by HPLC with photodiode array UV detector (260 nm). Results are expressed as means and SEM of values obtained from three independent experiments. Asterisks indicate significant difference compared with control (*$p < 0.05$, **$p < 0.01$) by Student's *t* test.

8-oxodG formation with increasing its concentration (1 μM; $p < 0.05$, 2 μM and higher; $p < 0.01$). Free nitrotyrosine induced the increase of 8-oxodG formation significantly at 10 μM ($p < 0.05$). Nitrotyrosine residue-containing histone-peptides induced 8-oxodG formation much more efficiently than free nitrotyrosine.

NADPH oxidation by nitrotyrosine in the presence of P450 reductase

NADPH oxidation to $NADP^+$ was analyzed by HPLC with photodiode array (Fig. 4). Free nitrotyrosine and nitroY-peptides significantly induced $NADP^+$ formation compared with control ($p < 0.05$ and $p < 0.01$, respectively). The amounts of $NADP^+$ by nitroY3-peptide and nitroY1-peptide were significantly higher than that of free nitrotyrosine ($p < 0.01$).

Discussion

The present study has demonstrated that nitrotyrosine and nitroY-peptides of histone have an ability to cause Cu(II)-mediated DNA damage via the activation with P450 reductase. Inhibitory effects of catalase and bathocuproine suggested that H_2O_2 and Cu(I) were required for DNA damage. A possible mechanism of

oxidative DNA damage induced by enzymatically activated nitrotyrosine can be speculated as accounting for most of the observations and references as follows. P450 reductase converts nitrotyrosine to corresponding nitro radical anion in the presence of NADPH via one-electron reduction [23,24]. The nitro radical anion reacts with O_2, followed by production of $O_2^{\cdot-}$ [25] and the consequent oxidation to the parent nitrotyrosine. Alternatively, there is a possibility that further nitroreduction by P450 reductase contributes to the generation of nitroso and/or *N*-hydroxy forms [26]. Any of reduced derivatives such as nitro radical anion, nitroso, and *N*-hydroxy forms may be oxidized again to yield redox cycle with generation of $O_2^{\cdot-}$. Subsequently, the generation of H_2O_2 by $O_2^{\cdot-}$ dismutation and reduction of Cu(II) to Cu(I) concomitantly occur. H_2O_2 reacts with Cu(I) to form a metal–oxygen complex such as Cu(I)-hydroperoxide causing DNA damage. This idea is supported by the observations that a typical free ·OH scavenger, ethanol, did not offer DNA protection. The complex DNA–Cu(I)–hydroperoxide may be considered to be a bound hydroxyl radical, which can release ·OH causing DNA damage. The ·OH released from the bound hydroxyl radical may immediately attack an adjacent constituent of DNA before it is scavenged by free ·OH scavengers [27]. NitroY-peptides damaged DNA more efficiently than free nitrotyrosine did. Relevantly, Krainev et al. [24] showed that nitrotyrosine residue within leucine enkephalin pentapeptide (Tyr–Gly–Gly–Phe–Leu) had a higher affinity for enzymatic reduction with higher production of $O_2^{\cdot-}$ than does free nitrotyrosine. We assessed the efficacy of redox cycling reaction by measuring $NADP^+$ as NADPH oxidation. The result also supported the idea that nitroY-peptides are more easily reduced by NADPH-P450 reductase than free nitrotyrosine. This can reasonably account for different DNA damaging potentials of free nitrotyrosine and nitrotyrosine-containing peptides.

It is considered that tyrosine plays a role in interactions of DNA-binding proteins and histones with DNA [28], probably through the close proximity of thymine and tyrosine in chromatin. Relevantly, Altman et al. [29] provided evidence for the formation of DNA–protein crosslinks between thymine and tyrosine in chromatin when cultured mannalian cells were treated with metal ions. When the tyrosine residues in histone are nitrated, reactive species derived from nitrotyrosine residue will immediately attack DNA. $ONOO^-$ is a potent DNA oxidizing agent [30], but it is very short-lived. On the other hand, nitrotyrosine has a long half-life in vivo. Nitrated proteins were detected for at least 24 h in rat skin singly exposed to $ONOO^-$ [31]. We have shown that enzymatically activated nitrotyrosine in histone peptide induced oxidative DNA damage in the presence of Cu(II). Abundant RNS are generated in inflammatory and infected tissues, and histone proteins are nitrated especially at tyrosine residues [14]. Most of nitrotyrosine in histone will be repaired by "denitrase" [15]. If nitrotyrosine residues still remain in histone, they may cause DNA damage in the presence of P450 reductase. This assumption is supported by the observation that P450 reductase exists in the nuclear fraction [32] although the amount of P450 reductase in nuclear fraction is smaller than that in cytosolic fraction. On the other hand, nitrotyrosine may be more easily catalyzed to reactive species by P450 reductase in cytosolic fraction. Therefore, both nitrotyrosines in cytosol and in nuclear histone may participate in DNA damage. In addition to the fact that nitrotyrosine is a marker for inflammation, we propose the possibility that nitrotyrosine-induced H_2O_2 formation and subsequent DNA damage contribute to inflammation-associated carcinogenesis.

Acknowledgment

This work was supported by a Grant-in-Aid from the Ministry of Education, Science, Sports and Culture of Japan.

References

[1] H. Ohshima, Genetic and epigenetic damage induced by reactive nitrogen species: implications in carcinogenesis, Toxicol. Lett. 140–141 (2003) 99–104.
[2] H. Ohshima, M. Tatemichi, T. Sawa, Chemical basis of inflammation-induced carcinogenesis, Arch. Biochem. Biophys. 417 (2003) 3–11.
[3] H. Wiseman, B. Halliwell, Damage to DNA by reactive oxygen and nitrogen species: role in inflammatory disease and progression to cancer, Biochem. J. 313 (1996) 17–29.
[4] S. Kawanishi, Y. Hiraku, M. Murata, S. Oikawa, The role of metals in site-specific DNA damage with reference to carcinogenesis, Free Radic. Biol. Med. 32 (2002) 822–832.
[5] S. Kawanishi, S. Inoue, S. Oikawa, N. Yamashita, S. Toyokuni, M. Kawanishi, K. Nishino, Oxidative DNA damage in cultured cells and rat lungs by carcinogenic nickel compounds, Free Radic. Biol. Med. 31 (2001) 108–116.
[6] H. Ischiropoulos, Biological selectivity and functional aspects of protein tyrosine nitration, Biochem. Biophys. Res. Commun. 305 (2003) 776–783.
[7] J.P. Eiserich, M. Hristova, C.E. Cross, A.D. Jones, B.A. Freeman, B. Halliwell, A. van der Vliet, Formation of nitric oxide-derived inflammatory oxidants by myeloperoxidase in neutrophils, Nature 391 (1998) 393–397.
[8] A. van der Vliet, J.P. Eiserich, H. Kaur, C.E. Cross, B. Halliwell, Nitrotyrosine as biomarker for reactive nitrogen species, Methods Enzymol. 269 (1996) 175–184.
[9] H. Ischiropoulos, Biological tyrosine nitration: a pathophysiological function of nitric oxide and reactive oxygen species, Arch. Biochem. Biophys. 356 (1998) 1–11.
[10] M.K. Shigenaga, H.H. Lee, B.C. Blount, S. Christen, E.T. Shigeno, H. Yip, B.N. Ames, Inflammation and NOx-induced nitration: assay for 3-nitrotyrosine by HPLC with electrochemical detection, Proc. Natl. Acad. Sci. USA 94 (1997) 3211–3216.

[11] L. Viera, Y.Z. Ye, A.G. Estévez, J.S. Beckman, Immunohistochemical methods to detect nitrotyrosine, Methods Enzymol. 301 (1999) 373–381.
[12] A. Ehsan, F. Sommer, A. Schmidt, T. Klotz, J. Koslowski, S. Niggemann, G. Jacobs, U. Engelmann, K. Addicks, W. Bloch, Nitric oxide pathways in human bladder carcinoma. The distribution of nitric oxide synthases, soluble guanylyl cyclase, cyclic guanosine monophosphate, and nitrotyrosine, Cancer 95 (2002) 2293–2301.
[13] A. Patel, C. Fenton, R. Terrell, P.A. Powers, C. Dinauer, R.M. Tuttle, G.L. Francis, Nitrotyrosine, inducible nitric oxide synthase (iNOS), and endothelial nitric oxide synthase (eNOS) are increased in thyroid tumors from children and adolescents, J. Endocrinol. Invest. 25 (2002) 675–683.
[14] A.S. Haqqani, J.F. Kelly, H.C. Birnboim, Selective nitration of histone tyrosine residues in vivo in mutatect tumors, J. Biol. Chem. 277 (2002) 3614–3621.
[15] Y. Irie, M. Saeki, Y. Kamisaki, E. Martin, F. Murad, Histone H1.2 is a substrate for denitrase, an activity that reduces nitrotyrosine immunoreactivity in proteins, Proc. Natl. Acad. Sci. USA 94 (2003) 5634–5639.
[16] P. Chumakov, EMBL Data Library, Accession No. X54156 (1990).
[17] M. Murata, S. Kawanishi, Oxidative DNA damage by vitamin A and its derivative via superoxide generation, J. Biol. Chem. 275 (2000) 2003–2008.
[18] M. Serrano, G.J. Hannon, D.A. Beach, A new regulatory motif in cell-cycle control causing specific inhibition of cyclin D/CDK4, Nature 366 (1993) 704–707.
[19] S. Oikawa, I. Hirosawa, K. Hirakawa, S. Kawanishi, Site specificity and mechanism of oxidative DNA damage induced by carcinogenic catechol, Carcinogenesis 22 (2001) 1239–1245.
[20] A.M. Maxam, W. Gilbert, Sequencing end-labeled DNA with base-specific chemical cleavages, Methods Enzymol. 65 (1980) 499–560.
[21] K. Ito, S. Inoue, K. Yamamoto, S. Kawanishi, 8-Hydroxydeoxyguanosine formation at the 5′ site of 5′-GG-3′ sequences in double-stranded DNA by UV radiation with riboflavin, J. Biol. Chem. 268 (1993) 13221–13227.
[22] A.J. Levine, J. Momand, C.A. Finlay, The p53 tumor suppressor gene, Nature 351 (1991) 453–456.
[23] T. Akaike, S. Okamoto, T. Sawa, J. Yoshitake, F. Tamura, K. Ichimori, K. Miyazaki, K. Sasamoto, H. Maeda, 8-Nitroguanosine formation in viral pneumonia and its implication for pathogenesis, Proc. Natl. Acad. Sci. USA 100 (2003) 685–690.
[24] A.G. Krainev, T.D. Williams, D.J. Bigelow, Enzymatic reduction of 3-nitrotyrosine generates superoxide, Chem. Res. Toxicol. 11 (1998) 495–502.
[25] M. Murata, M. Kobayashi, S. Kawanishi, Nonenzymatic reduction of nitro derivative of a heterocyclic amine IQ by NADH and Cu(II) leads to oxidative DNA damage, Biochemistry 38 (1999) 7624–7629.
[26] V.M. Arlt, H. Glatt, E. Muckel, U. Pabel, B.L. Sorg, A. Seidel, H. Frank, H.H. Schmeiser, D.H. Phillips, Activation of 3-nitrobenzanthrone and its metabolites by human acetyltransferases, sulfotransferases and cytochrome P450 expressed in Chinese hamster V79 cells, Int. J. Cancer 105 (2003) 583–592.
[27] M. Dizdaroglu, G. Rao, B. Halliwell, E. Gajewski, Damage to the DNA bases in mammalian chromatin by hydrogen peroxide in the presence of ferric and cupric ions, Arch. Biochem. Biophys. 285 (1991) 317–324.
[28] A. Zweidler, Role of individual histone tyrosines in the formation of the nucleosome complex, Biochemistry 31 (1992) 9205–9211.
[29] S.A. Altman, T.H. Zastawny, L. Randers-Eichhorn, M.A. Cacciuttolo, S.A. Akman, M. Dizdaroglu, G. Rao, Formation of DNA–protein cross-links in cultured mammalian cells upon treatment with iron ions, Free Radic. Biol. Med. 19 (1995) 897–902.
[30] S. Inoue, S. Kawanishi, Oxidative DNA damage induced by simultaneous generation of nitric oxide and superoxide, FEBS Lett. 371 (1995) 86–88.
[31] S.A.B. Greenacre, P. Evans, B. Halliwell, S.D. Brain, Formation and loss of nitrated proteins in peroxynitrite-treated rat skin in vivo, Biochem. Biophys. Res. Commun. 262 (1999) 781–786.
[32] M. Montalto de Mecca, E.G. Diaz, J.A. Castro, Nifurtimox biotransformation to reactive metabolites or nitrite in liver subcellular fractions and model systems, Toxicol. Lett. 136 (2002) 1–8.

Available online at www.sciencedirect.com
SCIENCE DIRECT
Mutation Research 558 (2004) 111–120
Genetic Toxicology and Environmental Mutagenesis
www.elsevier.com/locate/gentox
Community address: www.elsevier.com/locate/mutres

Metal-mediated oxidative damage to cellular and isolated DNA by gallic acid, a metabolite of antioxidant propyl gallate

Hatasu Kobayashi [a], Shinji Oikawa [a], Kazutaka Hirakawa [b], Shosuke Kawanishi [a,*]

[a] *Department of Environmental and Molecular Medicine, Mie University School of Medicine, Edobashi 2-174, Tsu, Mie 514-8507, Japan*
[b] *Department of Radiation Chemistry, Life Science Research Center, Mie University, Edobashi 2-174, Tsu, Mie 514-8507, Japan*

Received 26 August 2003; received in revised form 18 November 2003; accepted 18 November 2003

Abstract

Propyl gallate (PG), widely used as an antioxidant in foods, is carcinogenic to mice and rats. PG increased the amount of 8-oxo-7,8-dihydro-2′-deoxyguanosine (8-oxodG), a characteristic oxidative DNA lesion, in human leukemia cell line HL-60, but not in HP100, which is hydrogen peroxide (H_2O_2)-resistant cell line derived from HL-60. Although PG induced no or little damage to ^{32}P-5′-end-labeled DNA fragments obtained from genes that are relevant to human cancer, DNA damage was observed with treatment of esterase. HPLC analysis of the products generated from PG incubated with esterase revealed that PG converted into gallic acid (GA). GA induced DNA damage in a dose-dependent manner in the presence of Fe(III)EDTA or Cu(II). In the presence of Fe(III) complex such as Fe(III)EDTA or Fe(III)ADP, GA caused DNA damage at every nucleotide. Fe(III) complex-mediated DNA damage by GA was inhibited by free hydroxy radical (•OH) scavengers, catalase and an iron chelating agent. These results suggested that the Fe(III) complex-mediated DNA damage caused by GA is mainly due to •OH generated via the Fenton reaction. In the presence of Cu(II), DNA damage induced by GA occurred at thymine and cytosine. Although •OH scavengers did not prevent the DNA damage, methional inhibited the DNA damage. Cu(II)-mediated DNA damage was inhibited by catalase and a Cu(I) chelator. These results indicated that reactive oxygen species formed by the interaction of Cu(I) and H_2O_2 participates in the DNA damage. GA increased 8-oxodG content in calf thymus DNA in the presence of Cu(II), Fe(III)EDTA or Fe(III)ADP. This study suggested that metal-mediated DNA damage caused by GA plays an important role in the carcinogenicity of PG.

Keywords: DNA damage; Propyl gallate; Gallic acid; 8-Oxo-7,8-dihydro-2′-deoxyguanosine; Reactive oxygen species; Copper; Iron

1. Introduction

Propyl gallate (PG) is widely used as an antioxidant in the food industry. PG has been investigated as a potential chemopreventive agent in several animal experiments [1–3]. Thus, PG is recognized as being the important synthetic antioxidant. In contrast, National Toxicology Program (NTP) reported that PG induced preputial gland tumors, islet-cell tumors of the pancreas, and pheochromocytomas of the adrenal glands in male rats [4]. PG also induced malignant lymphoma

Abbreviations: PG, propyl gallate; 8-oxodG, 8-oxo-7,8-dihydro-2′-deoxyguanosine (also known as 8-hydroxy-2′-deoxyguanosine); GA, gallic acid; CIP, calf intestine phosphatase; DTPA, diethylenetriamine-*N*,*N*,*N*′,*N*″,*N*″-pentaacetic acid; DMSO, dimethylsulfoxide; BAP, bacterial alkaline phosphatase; SOD, superoxide dismutase; HPLC-ECD, an electrochemical detector coupled to high-performance liquid chromatography; HOMO, highest occupied molecular orbital

* Corresponding author. Tel.: +81-59-231-5011; fax: +81-59-231-5011.
E-mail address: kawanisi@doc.medic.mie-u.ac.jp (S. Kawanishi).

1383-5718/$ – see front matter © 2003 Elsevier B.V. All rights reserved.
doi:10.1016/j.mrgentox.2003.11.002